



Nanoscale

**Pore Surface Engineering of Covalent Organic Frameworks:
Structural Diversity and Applications**

Journal:	<i>Nanoscale</i>
Manuscript ID	NR-REV-08-2019-007525.R1
Article Type:	Review Article
Date Submitted by the Author:	26-Oct-2019
Complete List of Authors:	Vardhan, Harsh; University of South Florida, Department of Chemistry Nafady, Ayman; King Saud University, Chemistry Department; College of Science, King Saud University, Chemistry Al-Enizi, Abdullah; King Saud University, Chemistry Ma, Shengqian; University of South Florida, Department of Chemistry

SCHOLARONE™
Manuscripts

Pore Surface Engineering of Covalent Organic Frameworks: Structural Diversity and Applications

Harsh Vardhan,^a Ayman Nafady,^b Abdullah M. Al-Enizi,^b and Shengqian Ma^{*a}

^aDepartment of Chemistry, University of South Florida, 4202 East Fowler Avenue, Tampa, Florida-33620, USA. E-mail: sqma@usf.edu Fax: +1-813-974 3203; Tel: +1-813-974 5217.

^bDepartment of Chemistry, College of Science, King Saud University, Riyadh 11451, Saudi Arabia.

ABSTRACT: Connecting molecular building blocks by covalent bonds to form extended crystalline structures has given sharp upsurge in the field of porous materials especially covalent organic frameworks (COFs), thereby translating the accuracy, precision, versatility of covalent chemistry from discrete molecules to two-dimensional and three-dimensional crystalline structures. COFs are crystalline porous frameworks prepared by a bottom-up approach from predesigned symmetric units with well-defined structural properties such as high surface area, distinct pores, cavity, channels, thermal and chemical stability, structural flexibility and functional design. Due to the tedious and few times impossible introduction of certain functionalities into COFs via *de novo* synthesis, pore surface engineering through judicious functionalization with range of functionalities under ambient or harsh condition using the principle of coordination chemistry, chemical conversion, building block exchange is of profound importance. In this review, we aim to summarize dynamic covalent chemistry, frameworks linkage in context of design features, different ways and perspective of pore surface engineering along with their versatile role in a plethora of applications such as biomedical, gas storage and separation, catalysis, sensing, energy storage and environmental remediation.

KEYWORDS: Covalent organic frameworks, Dynamic linkage, Pore surface engineering, Biomedical, Gas storage and separation, Catalysis, Sensing, Energy storage, Environmental remediation.

INTRODUCTION: The utilization of confined space for molecular purpose is one of the basic principles of living systems and profoundly believed to be one of the vital steps in the origin of life. The biological process proceeds in spatial confinement commonly known as enzyme pocket drastically influence the reactivity and selectivity of biochemical reactions. To mimic this, linking organic building blocks by strong covalent bonds to form crystalline materials is vital however, one cannot neglect the possibility of thermodynamically favored amorphous disordered structure^{1,2}. In comparison to non-porous materials, porous materials gifted with various characteristics such as high surface area, nanometer-scale pores with peculiar properties and functions, tunable pore size, chemical and thermal stability³⁻¹¹. Covalent organic frameworks (COFs) are porous, crystalline extended solids constructed from organic building units entirely composed of light elements (C, H, N, B, O) and connected by covalent bonds which is robust and diverse in nature¹²⁻¹⁹. The strength of covalent bonds is unambiguously reflected in the giant structure of Vitamin B12 and other solid network in nature²⁰⁻²², in 2005, a revolution was made by successful connecting boronic acid and catechol to form extended structures⁶ using the principle of dynamic covalent chemistry^{23,24}. Since then, the sustained expansion and development of COFs are consequences to both long-lasting and newly recognized problems demanding new and evolving synthetic routes, characterization and applied studies.

The development of elementary skeletons in frameworks primarily relies on the geometry of building blocks. In 2D COFs, the building blocks are covalently bonded with a well-defined

stacking of π -building units under the influence of π - π stacking interactions whereas, the lattice structure of 3D COFs are preserved by robust covalent bond between precursor units using the principle of reticular chemistry²⁵⁻²⁹. The uniquely confined nanometer size pores have practical implementation as an outstanding platform for future challenges. With this goal in mind, it is important to examine the peculiar properties of COFs, starting with crystallinity. Due to the ordered structure, it enables characterization using powder X-ray diffraction pattern (PXRD), secondly, the porous nature arose from crystalline nature, uniform and periodic assembly of monomer units exhibit surface area as high as $4000 \text{ m}^2\text{g}^{-1}$, thirdly, chemical / thermal stability ($>400^\circ\text{C}$), emerge from robust and diverse nature of covalent bonds showed hinderance in severe conditions such as hydrolysis, oxidation, reduction, pH range, lastly, low density, by virtue of uniform composition with lightweight elements offer high gravimetric performance. *De novo* synthesis to lesser extent suffer with various challenges, such as active metal complexation, chemical conversion, tedious synthetic and purification procedure, etc. However, to address these challenges the tunable pore size of pristine frameworks undergoes pore surface engineering using the established molecular organic chemistry to tune structural and functional properties of COFs to address challenging issues. In this review, we will briefly mention the extraordinary role of dynamic covalent chemistry in synthesizing COFs of specific pore size and broadly summarize the principle and examples of pore surface engineering in framework along their role in vast number of applications such as drug delivery, catalysis, environmental remediation, gas adsorption and separation, sensing and energy storage.

DYNAMIC LINKAGES: Since the advent of first COF in 2005, the last decade has observed substantial development in COFs from designing, constructing and application viewpoint. There are range of linkages as shown in Figure 1 employed to construct extended frameworks of different

pore structure and morphologies. Different from traditional interactions, dynamic covalent bonds possess error-checking capability and robustness of reversible bonds at the same time bestow COFs with thermal stability, crystallinity, diversity, etc. The chemical stability and crystallinity are two peculiar properties which are dependent and comes with the expense of others. In recent years, numerous thematic perspectives and reviews discussed^{16, 30-37} in great detail the role of dynamic covalent chemistry in constructing framework of different linkages under the umbrella of reticular chemistry and their implementation in different pore size, pore volume and dual pore framework. So, we are not trying to duplicate those aspects however, briefly highlighted different linkages and pore geometry present in the COFs to create cohesion for the better understanding of central theme of this review.

B—O Linkages: Yaghi and co-workers reported first class of boroxine-based frameworks^{6,38} (COF-1, COF-102) by self-condensation of boronic acid-based building unit and co-condensation of same building block with catechol generate boronate ester linkage framework (COF-5, COF-105). Due to the vulnerability of B—O linkage, the frameworks hydrolyzed in moisture. Furthermore, Dichtel research group also highlighted the dissociation of HHTP-DPB COF in aqueous solution within minutes³⁹. To enhance the stability, Yaghi's group introduced B—O—Si linkage in borosilicate-linked framework (COF-202) prepared by reaction of silanols with boronic acid showing stability in moisture from minutes to days⁴⁰. Additionally, the stability of frameworks in water and basic medium visualized in spiroborate-linked ionic COFs by varying the hybridization of boron by incorporating alkali metal ions⁴¹.

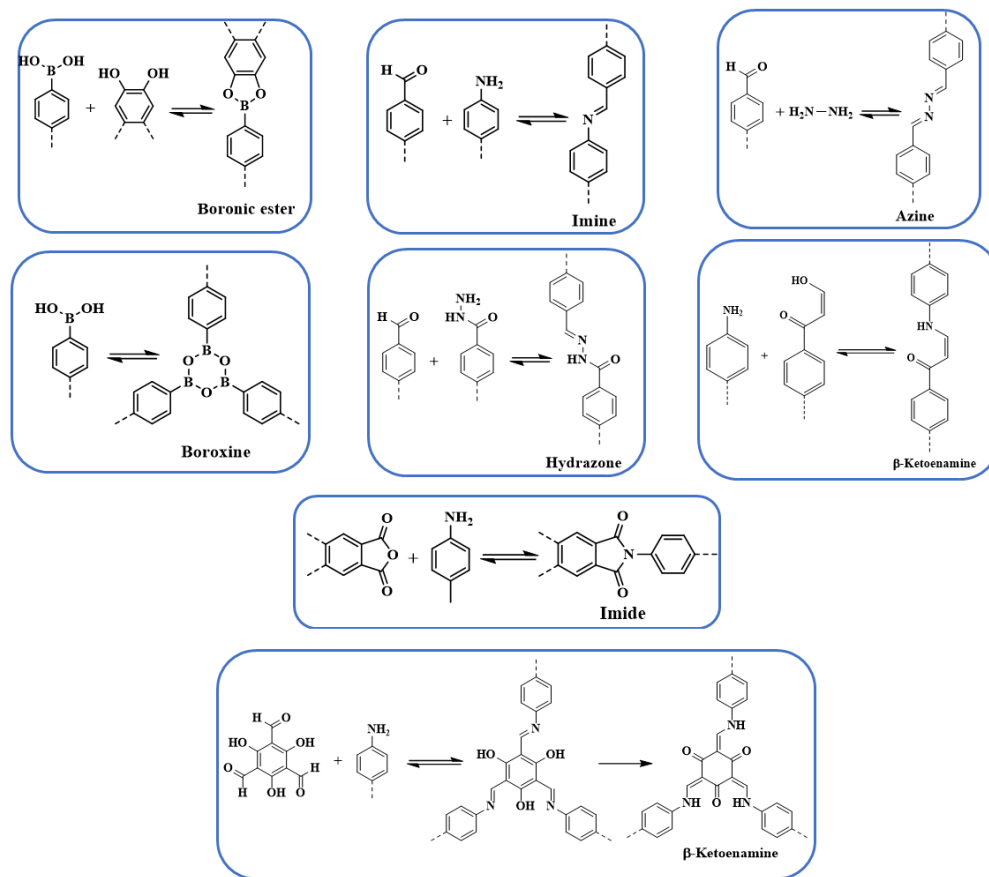


Figure 1. Different condensation reactions used for COFs synthesis.

C—N Linkages: Yaghi research group designed COF-300 by using dynamic imine linkage, which in comparison to boron-linked framework, exhibited higher stability in water, protic, aprotic solvents and entire pH range⁴². To further elevate the stability of imine-based COFs, Banerjee and co-workers reported⁴³ TpPa-1 and TpPa-2 by reaction of 1,3,5-triformylphloroglucinol with *p*-phenylenediamine and 2,5-dimethyl-*p*-phenylenediamine respectively. The stability mainly arose from aldimine condensation followed by irreversible tautomerism from enol-imine to keto-enamine⁴⁴⁻⁴⁶. Jiang research group reported^{47,48} azine-linked framework (-C=N-N=C-) by condensation reaction of azine and formyl substituted scaffold. In recent years, squaraine-based

and violagen-based COFs were also reported to highlight the pivotal importance of C—N linkages⁴⁹.

C—C Linkages: Hecht research group⁵⁰ reported first ever C—C linked framework using Ullmann coupling reaction and thereafter Knoevenagel condensation employed to construct framework⁵¹⁻⁵⁵. Jiang and co-workers synthesized sp^2 carbon-conjugated framework by condensation of nitrile functionalized precursor such as 1,4-phenylenediacetonitrile with formyl substituted monomer⁵⁶. Recently, Yaghi's group reported -C=C- linked framework by condensation of 2,4,6-trimethyl-1,3,5-triazine (TMT) and 4,4'-biphenyldicarbaldehyde (BPDA) via Aldol condensation with an extraordinary stability in Brønsted acid or base⁵⁷.

Apart from these commonly used linkages in constructing COFs, borazine-, azodioxide- and hetero-linked frameworks were also reported⁵⁸⁻⁶¹. In addition to the linkage used to construct framework, synthetic methods such as solvothermal^{38,42}, ionothermal⁶², microwave^{63,64}, mechanochemical^{45,46}, interfaces^{65,66}, room temperature^{67,68} also plays pivotal impact in synthesis and various properties such as crystallinity, surface area of synthesized frameworks.

PORE DESIGN: Reticular chemistry goes back to the work first highlighted by noble laureate Alfred Werner⁶⁹ in discovering complex such as $\beta\text{-Co(4-methylpyridine)}_4(\text{NCS})_2$ and later in 1959 first crystalline coordination networks reported with metal-neutral ligand linkage^{70,71}. The reticular chemistry implements in COFs from two standpoints, first, the backbone of framework and second the space comprised by the framework. These outlooks primarily depend on linkage and symmetry of building units as shown in Figure 2. The systematic pore network in COFs assist inclusion of various guest molecules under non-covalent interaction, therefore, geometrical configuration of building blocks is of profound importance to translates the shape and size

selective ingress of molecules. Jiang's group underlined the relationship between the pore structure and building units in a topological diagram, hexagonal, tetragonal, trigonal and rhombic structures have been widely employed^{30,72}. COF-6 exhibited smallest pore (0.87 nm)⁷³ whereas, PC-COF in 2016 showed largest pore (5.8 nm) reported so far⁷⁴.

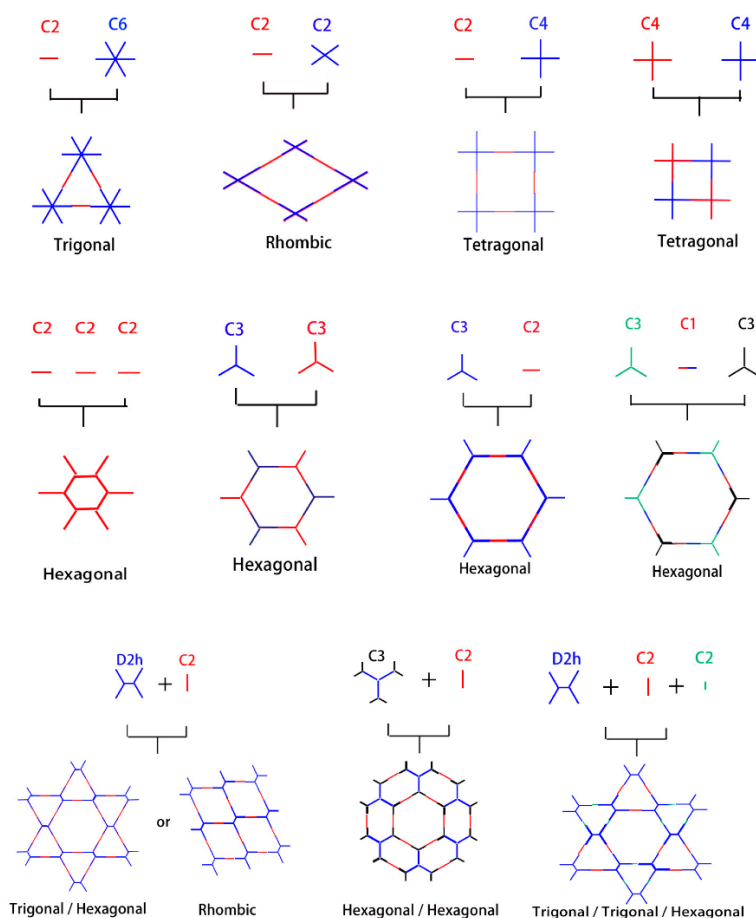


Figure 2. Organic building block geometries and the resulting COFs structural pattern.

Reproduced with permission from ref. 35. (Copyright © 2018, MDPI)

In addition to this, significant large pores highlighted so far are HHTP-DPB COF³⁹ (4.7 nm), BTP-COF⁶⁴ (4.0 nm), D_{TP}-ANDI COF⁷⁵ (5.3 nm). The tunable pore size of framework highlighted by Lavigne research group⁷⁶ by incorporating methyl, ethyl and propyl functionalities

into framework experienced substantial decrease in surface area and pore size to 1.6 nm, 1.4 nm and 1.1 nm respectively, thereby, implying decrease in pore size is directly proportional to the size of substituents (-Me < -Et < -Pr). Jiang and co-workers further highlight alkenyl, alkynyl, azide-decorated framework and observed decrease in pore size in comparison to pristine frameworks⁷⁷. Moreover, Zhao research group⁷⁸ reported dual pore and three different kind of pores by using D_{2h} symmetric 4,4',4'',4'''-(ethane-1,1,2,2-tetrayl) tetraaniline building block (ETTA). Along with this, Yaghi, Wang and other research group reported heterogeneous pore structure and variation of pore shape with change in building block concentration⁷⁹⁻⁸⁴.

CHARACTERIZATION: COFs synthesized by different methodologies typically characterized using diverse physiochemical techniques to determine and understand their properties. The range of techniques widely used for the characterization of frameworks are briefly describe, starting with powder X-ray diffraction (PXRD), PXRD are performed to determine the bulk crystallinity of frameworks. The structure identification can be done by comparing the experimental diffractogram of the frameworks with pattern calculated using the AA stacking and AB stacking model generated by the computational modeling. The model structure undergoes Pawley refinement to optimize the lattice parameters iteratively until R_{WP} value converges, thereby, provide crystallographic parameters such as lattice parameters, unit cell and make it possible to distinguish between amorphous and crystalline material. This is basic characterization, yet of profound importance and extensively used to verify the synthesis of existed and novel COFs. Secondly, nitrogen adsorption and desorption isotherms, the pore volume, pore size distribution, surface area are various parameters determined by N_2 adsorption isotherm at 77 K. To investigate these textural parameters, the sample should be properly activated. In general, porous materials are usually activated by Soxhlet extraction, solvent exchange, supercritical drying and vacuum drying. Furthermore, the

amount of sample is of key importance, to get infallible data, the weight of sample (g) multiplied by the specific surface area (m^2g^{-1}) should be equal to 100 m^2 or more. In general, the physisorption isotherms divided into six types of different shapes implying either micropores, mesopores or macropores. Thirdly, thermogravimetric analysis (TGA) measure the mass loss as a function of temperature in a controlled atmosphere. This technique helps in determining the thermal stability of the COFs, for instance, TGA data of imine-linked frameworks usually indicates thermal stability up to $350 \text{ }^\circ\text{C}$. Generally, the weight loss of the COFs vs temperature ($^\circ\text{C}$) highlights solvent molecule loss at $50\text{-}100 \text{ }^\circ\text{C}$ and second loss implies to structural modification and collapse of frameworks ($350\text{-}450^\circ\text{C}$). Fourthly, scanning electron microscopy (SEM) and transmission electron characterization (TEM) are used to examine the morphology, dispersion and mixture of phases and particle size of frameworks. The sample underwent pretreatment by gold coating the surface of conducting materials before SEM analysis. These microscopies can be coupled with Energy Dispersive Spectroscopy (EDS) or Energy Dispersive X-ray Analysis (EDX), which helps in determining the elemental quantitative and qualitative composition of COFs. Fifthly, ^{13}C cross polarization magic-angle spinning (CP-MAS) used to determine the COFs purity and unreacted organic linkers. This helps in elucidating the structure, identity or chemical state of frameworks, for instance, imine-linked frameworks showed -C=N moieties at 159 ppm in ^{13}C MAS NMR. These observations were further confirmed by using Fourier Transform-Infrared Spectroscopy (FT-IR), by emergence of imine functionalities and disappearance of carbonyl moieties. Lastly, aqueous and chemical stability of COFs, to test the stability the thumb rule is soaked the COFs in water, protic, aprotic, acidic and basic pH solutions for requisite amount of time. The solution is left undisturbed at specific temperature and time followed by filtration and reactivation and compared material with pristine frameworks by means of PXRD, FT-IR and surface area

measurements. Depending on the nature of COFs, Ultraviolet-Visible Spectroscopy, Inductively Coupled Plasma Optical Emission Spectroscopy (ICP-OES) and photoluminescence spectroscopy techniques are also widely used.

PORE SURFACE ENGINEERING: The robust interaction between uniformly distributed binding functionalities in COFs and metal ions such as Pd, V, Rh, Re, Cu under the principle of coordination chemistry is one of the common ways to impart catalytically active moieties in frameworks. COFs with bipyridine, bicatechol moieties are at the forefront of linking metal ions due to their donor ability to form σ dative bond. It is worth to point out that metal binding in between the nitrogen (Schiff base COFs) of the adjacent layers of the framework further helps in considerable increment of active catalytic sites. The functional groups directly linked to the organic scaffold provide anchimeric assistance along with imine nitrogen to combine with foreign species which includes well-known systems such as iminophenol, benzoyl hydrazone, salen, β -ketoenamine, etc. In addition to this, porphyrin incorporated frameworks bestow with inherent coordinative, redox and spectral features. The presence of four pyrrolic units bind with most elements present in the periodic table^{85,86}, Fe-porphyrin and Co-porphyrin-based COFs, for instance showed peroxidase-like activity⁸⁷ and electrocatalytic reduction of CO₂⁸⁸ respectively. Planar triangular macrocycle such as dehydrobenzoannulene derivatives (DBAs) are well-known to bind with low oxidation state transition metals⁸⁹. DBA being neutral and possess soft binding functionalities (alkyne) as compared to hard nitrogen atoms has different reaction pattern under the HSAB rule, for instance, DBA-based COFs metalated with Ni(0) exhibited hybrid material with an exceptional uptake of ethylene and ethane⁹⁰.

Imine-linked frameworks are at the forefront to study pore surface engineering due to an extraordinary thermal and chemical stability in moisture, protic and aprotic solvent. Wang research group synthesized⁹¹ two-dimensional COF-LZU1 by condensation of 1,3,5-triformylbenzene and *p*-phenylenediamine in presence of acetic acid demonstrate excellent crystallinity and surface area ($410 \text{ m}^2\text{g}^{-1}$). COF-LZU1 adopt eclipsed structure with adjacent layer distance of 0.37 nm susceptible for binding with palladium acetate, Pd/COF-LZU1 (Figure 3), well-preserved crystalline framework showed small decrease in surface area and 0.7 eV negative shift in X-ray photoelectron spectroscopy (XPS) in comparison to 338.4 eV for free Pd(OAc)₂. These results in totality affirm the pore surface engineering with a regular channel diameter of 1.8 nm, exposed to ingress of electronically and sterically bulky molecules for Pd/COF-LZU1 catalyzed Suzuki-Miyaura coupling reactions in an extraordinary yield of 96% to 98% with an excellent recyclability and reusability. Five years later, Li research group used same hybrid material, Pd/COF-LZU1 annealed at 500 °C to generate palladium nanoparticles encapsulated in the shell of the nitrogen doped hollow carbon material⁹². Pd(0) hybrid framework with similar morphology serve as an efficient catalyst for hydrogenation of nitroaromatics to amine which is far superior to Pd(0) and other commercial carbon material.

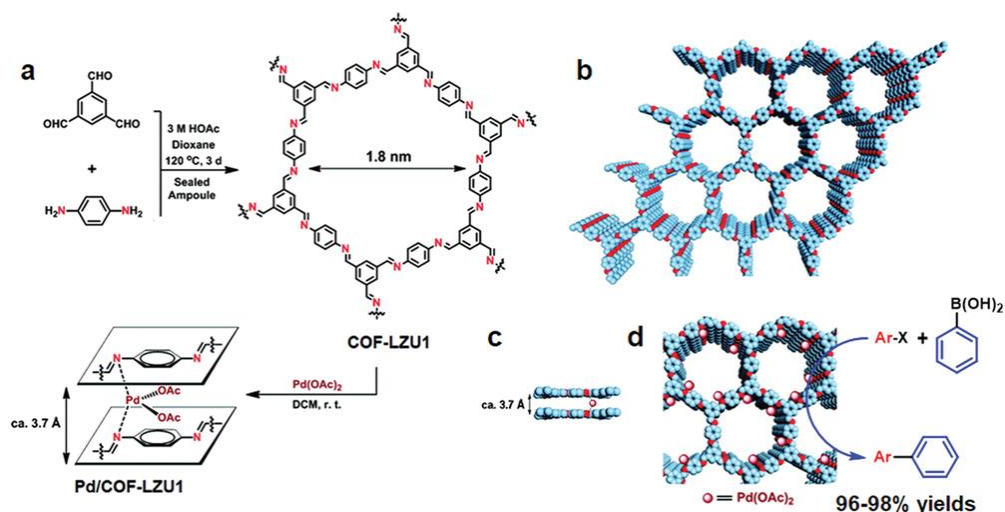


Figure 3. a.) COF-LZU1 and Pd/COF-LZU1 synthesis. b-d.) Proposed 2D COF-LZU1 and Pd/COF-LZU1 layered structures with Pd immobilization. Adapted with permission from ref. 91.

(Copyright © 2011, American Chemical Society)

In 2018, Kim research group combined the chemistry of two porous materials, -NH_2 functionalized MOF and COF-LZU1 with impregnation of $\text{Pd}(\text{OAc})_2$. XPS spectrum showed the binding of palladium with imine nitrogen very similar to Pd/COF-LZU1, the hybrid $\text{Pd}^{2+}/\text{MOF}@\text{COF}$ material exhibit photocatalytic tandem dehydrogenation and hydrogenation reactions⁹³. Sticking to the pore surface engineering of COFs with palladium, Jiang research group reported successful immobilization of palladium into porphyrin containing imine-linked COF and employed as effective Suzuki-coupling reaction under mild condition in 97%-99% yield⁹⁴. Gao and co-workers demonstrate accuracy and precision control on the number and position of catalytically active centers. To highlight this control⁹⁵, Py-2,2'-BPyDCA COF synthesized by condensation of 4,4',4'',4'''-(pyrene-1,3,6,8-tetrayl) tetraaniline (PyTTA) and 2,2'-bipyridine-5,5'-dicarbaldehyde (2,2'-BPyDCA) / 4,4'-biphenyldialdehyde in different stoichiometric ratio. Using this planned synthetic method, first, bulky $\text{Rh}(\text{COD})\text{Cl}$ ($7.4 \times 6.6 \times 5.3 \text{ \AA}$) coordinated with bipyridine functionalities followed by palladium resulting bimetallic $\text{Rh}^{\text{I}}/\text{Pd}^{\text{II}}@\text{BPy-COF}$ for one-pot addition-oxidation cascade reactions (Figure 4). Using the same principle, similar bimetallic framework prepared by docking MnCl_2 followed by $\text{Pd}(\text{OAc})_2$ to Py-2,2'-BPyDCA COF afford $\text{Mn}^{\text{II}}/\text{Pd}^{\text{II}}@\text{BPyCOF}$ with Mn(II) and Pd(II) content of 7.9 wt% and 0.8 wt% respectively catalyzed Heck reaction between styrene and iodobenzene and subsequent epoxidation of *trans*-stilbene to *trans*-stilbene oxide⁹⁶.

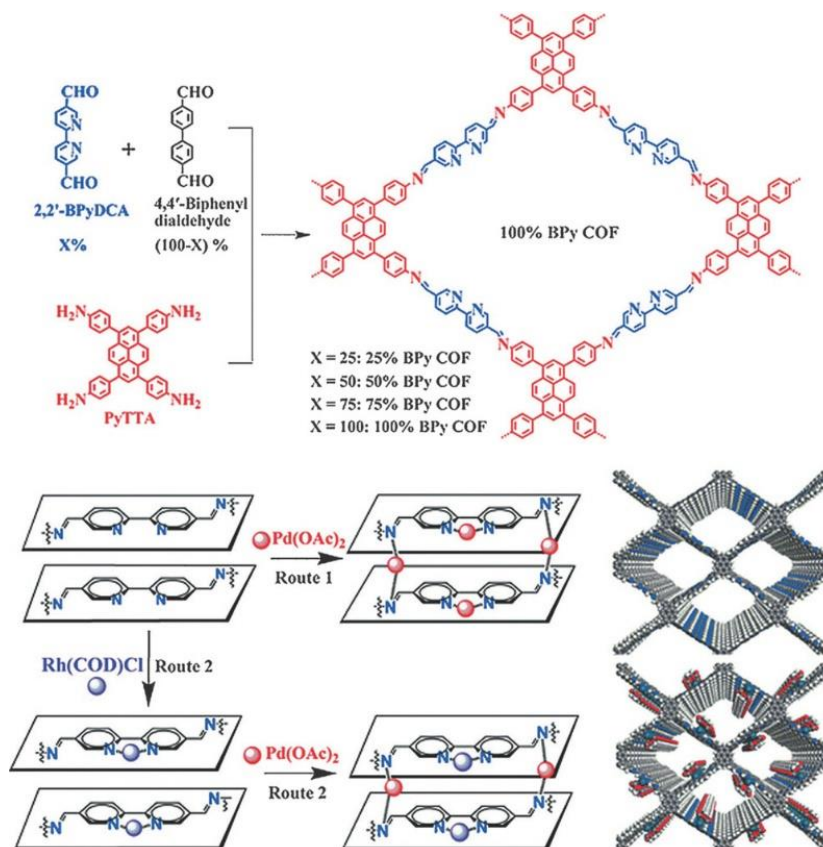


Figure 4. Synthesis of $X\%$ -BPy COFs and routes of pore surface engineering with rhodium and palladium. Reproduced with permission from ref. 95. (Copyright © 2016, Wiley-VCH Verlag

GmbH & Co. KGaA, Weinheim)

Pd(II)/COF-SDU1 synthesized by palladium-based pore surface engineering of SDU1 framework prepared by condensation of 1,4-phenylenediamine and tri(4-formacylphenoxy)-1,3,5-triazine. The hybrid framework characterizes using physiochemical analysis and employed as an effective heterogeneous catalyst for one-pot cross coupling reaction between phenylsilane and range of electronically substituted iodotoluene with excellent recyclability⁹⁷. Pachfule *et al.* reported in situ generation of Pd nanoparticle in the pores of β -ketoenamine TpPa-1 COF constructed by condensation of 1,3,5-triformylphloroglucinol and 1,4-phenylenediamine. The hybrid Pd(0)@TpPa-1 catalyze coupling reactions, one-pot sequential Heck Sonogashira coupling

reaction and intramolecular oxidative coupling⁹⁸. Iron, cobalt and nickel are among other transition metal ions incorporated into COFs through systematic pore surface engineering. RT-COF-1 synthesized⁹⁹ by the reaction of 1,3,5-tris(4-aminophenyl) benzene and 1,3,5-benzenetricarbaldehyde at ambient temperature in *m*-cresol. The treatment of RT-COF-1 with M(acac)_n {M = Fe(III), Co(II), Ni(II); acac = acetylacetonate) in methanol at room temperature for 24 hours produce metal incorporated framework with different metal to nitrogen ratio. As shown by total X-ray fluorescence (TXRF), atomic ratio of Fe^{III} : N, Co^{II} : N, Ni^{II} : N is 1:280, 1:190 and 1:760 respectively, which is smaller than Pd, Rh, Mn docked frameworks¹⁰⁰. The dramatic fluorescence quenching after metal docking owing to metal-to-ligand charge transfer further affirm the successful immobilization. Banerjee research group reported¹⁰¹ cobalt immobilization in β-ketoenamine linked COF-TpBpy prepared by condensation reaction of 5,5'-diamino-2,2'-bipyridine and 1,3,5-triformylphloroglucinol. The solution-infiltration way of pore surface engineering imparts ~12% cobalt content as investigated by ICP-OES. XPS, EDX, FT-IR analysis further confirm the coordination of cobalt species to bipyridine moieties without any proof of linking with imine nitrogen. Crystalline Co-TpBpy framework with accessible surface area of 450 m²g⁻¹ acts as OER catalyst up to 1000 cycles. Same framework was used by our research group¹⁰² to highlight the role of degree of freedoms within the pore channel of framework to accommodate linear ionic polymer and active Lewis acidic copper sites (Figure 5). The two reactive centers in hybrid PPS□COF-TpBpy-Cu works concerted for effective catalytic conversion of sterically and electronically substituted epoxide to cyclic carbonate using CO₂ in comparison to pristine framework, ionic polymer or copper salt. The boosting cooperation remained active in hybrid framework even after ten catalytic cycle without any drastic change in activity and crystallinity.

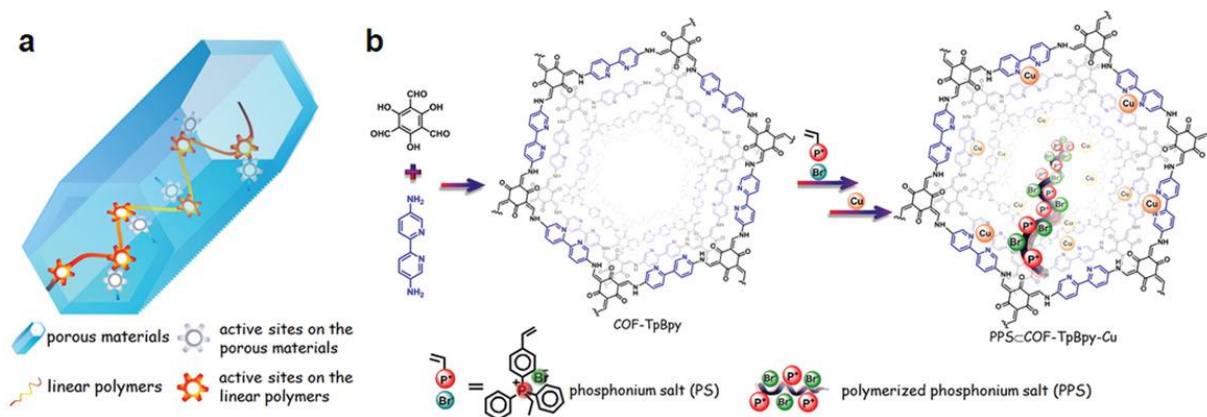


Figure 5. Porous heterogeneous concerted catalyst with flexible polymer and metal active sites;
b.) Schematic presentation of PPS-COF-TpBpy-Cu synthesis from COF-TpBpy, PPS and Cu.

Adapted with permission from ref. 102. (Copyright © 2016, American Chemical Society).

The pivotal role of bipyridine functionalities in imine-linked COFs for pore surface engineering is extraordinary, similar attention was also drawn by the pendant hydroxyl groups attached to the building blocks distributed uniformly in the COFs. Chen and co-workers¹⁰³ synthesized hydroxyl functionalized crystalline and porous framework by dynamic imine linkage of 2,5-dihydroxyterephthalaldehyde and 1,3,5-tris(4-aminophenyl) triazine in *o*-dichlorobenzene, *n*-butanol and catalytic amount of 3M acetic acid. Due to the presence of pendant moieties and stacked structures, the authors further illustrated pore surface engineering using Cu(OAc)₂ with Cu(II) coordinated with dangling hydroxyl groups and imine nitrogen with similar coordination environment extensively reported in homogenous counterparts. Cu-COF explored as heterogeneous catalyst for selective oxidation of alkene in presence of hydroperoxide with more than 75% conversion and can be reusable for at least three catalytic cycle without any significant change in crystallinity and morphology. Salen-based ligands have special place in the field of coordination chemistry^{104, 105}, Ding, Wang and co-workers illustrate the incorporation of these moieties in COFs by synthesizing Salen-COF via condensation of ethylene diamine and C₃

symmetric 1,3,5-tris[(5-tert-butyl-3-formyl-4-hydroxyphenyl)ethynyl] benzene. The crystalline nature of framework is well-preserved in entire pH range, protic and aprotic solvents, furthermore, salen pockets in pore channel underwent pore surface engineering using $\text{Co}(\text{OAc})_2$, $\text{Cu}(\text{OAc})_2$, $\text{Ni}(\text{OAc})_2$, $\text{Zn}(\text{OAc})_2$ and $\text{Mn}(\text{OAc})_2$ to form metallo-salen-based COFs. Co/Salen COF exhibited excellent catalytic activity for Henry reaction using nitro alkane and aldehyde or ketone in presence of base with recyclability and reusability up to four catalytic cycles¹⁰⁶. Our research group demonstrated vanadium docking in catechol functionalized TAPT-2,3-DHTA framework by reaction of $\text{VO}(\text{acac})_2$ in THF at 50 °C (Figure 6). Electron paramagnetic resonance (EPR) spectroscopy and XPS affirm vanadium immobilization in VO-TAPT-2,3-DHTA COF with no change in crystallinity and surface area of $562 \text{ m}^2\text{g}^{-1}$. The recyclable hybrid material exhibited catalytic activity for Prins reaction (nopol formation) and substituted sulfide oxidation with 69% and 90% yield respectively¹⁰⁷. Moreover, VO-TAPT-2,3-DHTA and VO-PyTTA-2,3-DHTA COFs demonstrate excellent catalytic efficiency for Mannich-type reaction with 75% - 99% yield for Mannich base formed from range of electronically and sterically substituted alcohol and 4-methylmorpholine *N*-oxide (NMO) / trimethylamine *N*-oxide (TMNO)¹⁰⁸.

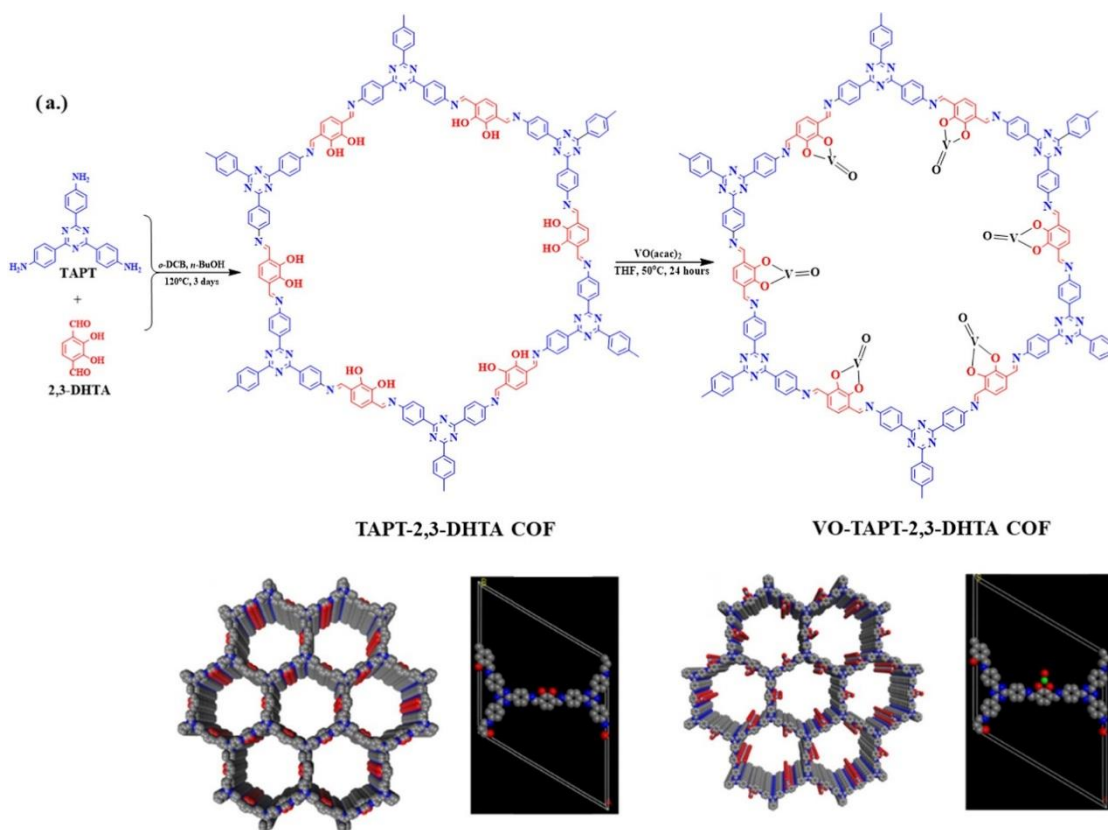


Figure 6. Synthesis and stacked structure of TAPT-2,3-DHTA COF and pore surface engineered VO-TAPT-2,3-DHTA COF. Reproduced with permission from ref. 107. (Copyright © 2019, American Chemical Society)

Planar and rigid nature of porphyrin building blocks with inherent abundantly functionalized nitrogen led to stabilized COFs due to π - π stacking interaction between adjacent layers. In 2017, Star research group⁸⁷ synthesized bifunctional Fe-DhaTph COF by two ways, first involves pre metalation of 5,10,15,20-tetrakis(4-aminophenyl) porphyrin with $\text{FeCl}_2 \cdot 2\text{H}_2\text{O}$ followed by condensation with 2,3-dihydroxyterephthalaldehyde, secondly, post metalation of DhaTph COF with Fe(III). Recently, Marinescu and co-workers synthesized bimetallic frameworks both pre and post metalation strategy, COF-Re prepared by dynamic imine linkage between Re-2,2'-BPyDCA and 5,10,15,20-tetrakis(4-aminophenyl) porphyrin, followed by pore

surface engineering using cobalt and iron chloride resulting COF-Re_Co and COF-Re_Fe respectively⁸⁸. PXRD pattern illustrate both bimetallic frameworks preserve crystallinity during modification, furthermore, XPS analysis revealed peaks for both metals present in the COFs highlighting successful incorporation of metals with distinct properties. With 53.4 wt% of cobalt in COF-Re_Co, the framework exhibited CO₂ reduction to CO with faraday efficiency of 18%. In addition, phenanthroline moieties in copper(I)-bisphenanthroline tetrafluoroborate and benzidine afford 3D COF-505 by mutual weaving at regular intervals¹⁰⁹. By definition, COFs composed of organic building blocks, therefore, pore surface engineering reflect in removal of copper ions by heating COF-505 in KCN CH₃OH-H₂O solution and found approximately 92%-97% removal as measured by ICP analysis (Figure 7). PXRD and SEM exhibited slight decrease in crystallinity and similar morphology in comparison to pristine framework, notably, the authors explained metalation and remetation, more importantly, this work provides alternative to porphyrin, bipyridine, hydroxyl moieties in front of COFs community. 3D metalated COFs restricted accessibility challenges in front of the chemists to produce symmetric monomers to form porous material with distinct properties. McGrier research group reported crystalline DBA-3D-COF by solvothermal reaction of dehydrobenzoannulene (DBA) and tetra(4-dihydroxyborylphenyl) methane gifted with uniformly distributed π -conjugated planar ring. The soft neutral π -ligands donate one-two electron pair per alkyne to form Ni-DBA-3D-COF with complete preservation of crystallinity. More importantly, XPS analysis exhibited nickel binding with the alkynyl units in zero oxidation state without any interaction with boronate ester linkages. In comparison to pristine framework, nickel metalated framework observed ethane and ethylene sorption of 0.07 mmol and 0.13 mmol at 295 K respectively⁹⁰.

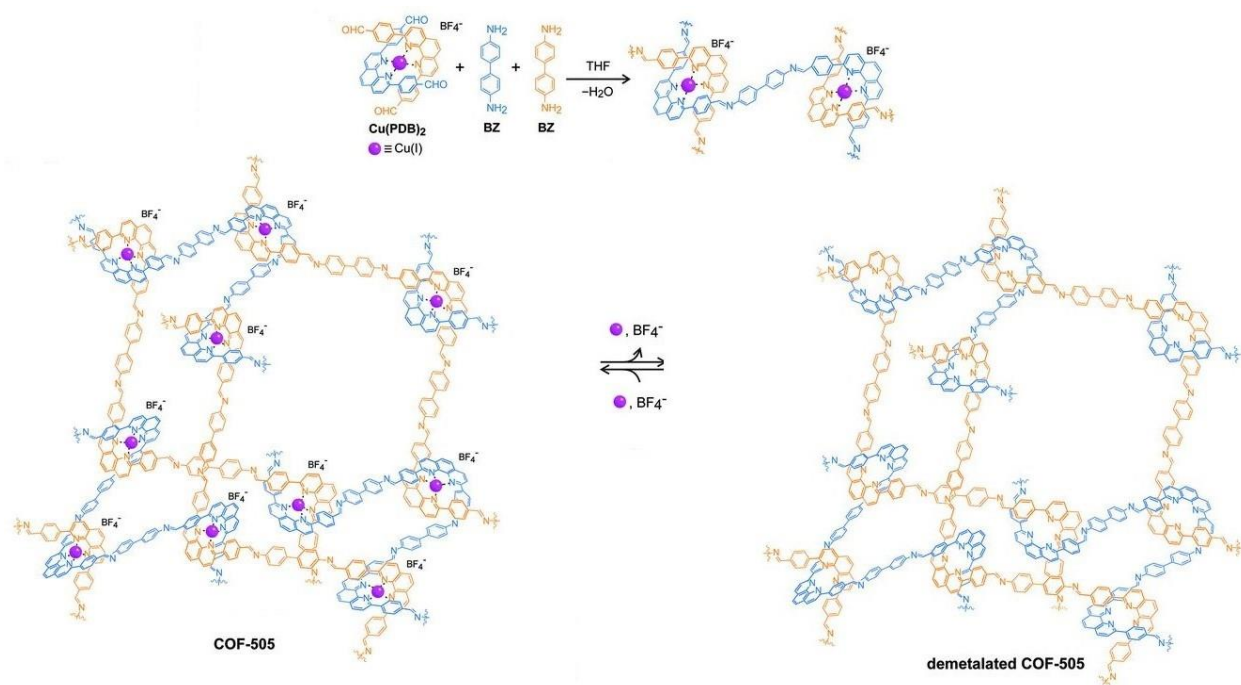


Figure 7. Synthesis of COF-505 from organic threads using Cu(I) as template to design extended weaving structure with demetalated and remetalted reversibility. Reprinted with permission from ref. 109. (Copyright © 2016, American Association for the Advancement of Science)

Extraordinary stability of β -ketoenamine COFs is extensively reported by Banerjee and co-workers, usually prepared by condensation of triformylphloroglucinol with range of substituted amines. Shen, Zhang and co-workers used structural and geometrical advantages of TpPa-2 COF⁴³ for pore surface engineering with Ti^{4+} using $\text{Ti}(\text{SO}_4)_2$. The physiochemical analysis showed complete retention of crystallinity, morphology with 33.49 wt% of titanium and the decorated TpPa-2- Ti^{4+} framework used for phosphopeptide enrichment using tryptic digests of standard phosphoprotein β -casein¹¹⁰. Our research group used β -ketoenamine COF prepared by condensation of triformylphloroglucinol and 2,5-diaminopyridine to examine cascade catalysis after successful pore surface engineering by palladium using $\text{Pd}(\text{OAc})_2$ (Figure 8). XPS revealed palladium coordination with pyridinic and secondary amine of linkages in the framework with

substantial weight percentage. The presence of two active palladium and basic nitrogen catalytic sites make the hybrid framework apt for cascade catalyst for oxidation-Knoevenagel condensation reaction from alcohols to unsaturated dinitriles with excellent recyclability¹¹¹. Yuan and Zhu group extend the principle of pore surface engineering to study gas adsorption behavior by synthesizing carboxyl functionalized framework. $\{(HOOC)_x\text{-COF}, X = 17, 33, 50 \text{ and } 100\}$ TpPa-COOH framework synthesized by condensation of 2,5-diaminoterephthalic acid, 1,4-phenyldiamine and triformylphloroglucinol in different ratio and compared with TpPa-1 prepared using 1,2-phenyldiamine. The presence of proton donating and proton accepting groups simultaneously for hydrogen bonding units reduce the ammonia uptake as compared to pristine framework due to decrease in pore size, furthermore, the functionalized framework on treatment with calcium chloride, manganese chloride and strontium chloride led to assimilate the metal ions at carboxyl moieties thereby, serve as open metal sites. This synergism positively influences the ammonia uptake with 14.3 mmol g^{-1} , 19.8 mmol g^{-1} at 298 K and 273 K respectively¹¹². In 2011, Yaghi and co-workers highlight first ever report of hydrazone linked stable COFs¹¹³, soon after, Jiang research group exemplified two-step bottom approach by pore surface engineering of frameworks synthesized by condensation of triformylphloroglucinol with terephthalohydrazide and substituted terephthalohydrazide using $\text{MoO}_2(\text{acac})_2$ ¹¹⁴. The salicylaldehyde benzoyl hydrazone strong coordination with molybdenum showed in XPS, FT-IR and TGA analysis. ICP analysis revealed 2.0 mmol g^{-1} density of molybdenum, which is susceptible to make framework catalytically active for epoxidation of cyclohexene in 99% conversion and up to 70% selectivity. Using the same principle Zhao research group used hydroxyl functionalized COFs synthesized by triformylphloroglucinol and 2,5-dihydroxyterephthalohydrazide or 2,3-dihydroxyterephthalohydrazide to incorporate cobalt in +2 oxidation state as evident by XPS,

TEM-elemental mapping and serve as Lewis acidic sites for cyanosilylation of electronically and sterically substituted aldehyde to form cyanohydrin with excellent recyclability¹¹⁵.

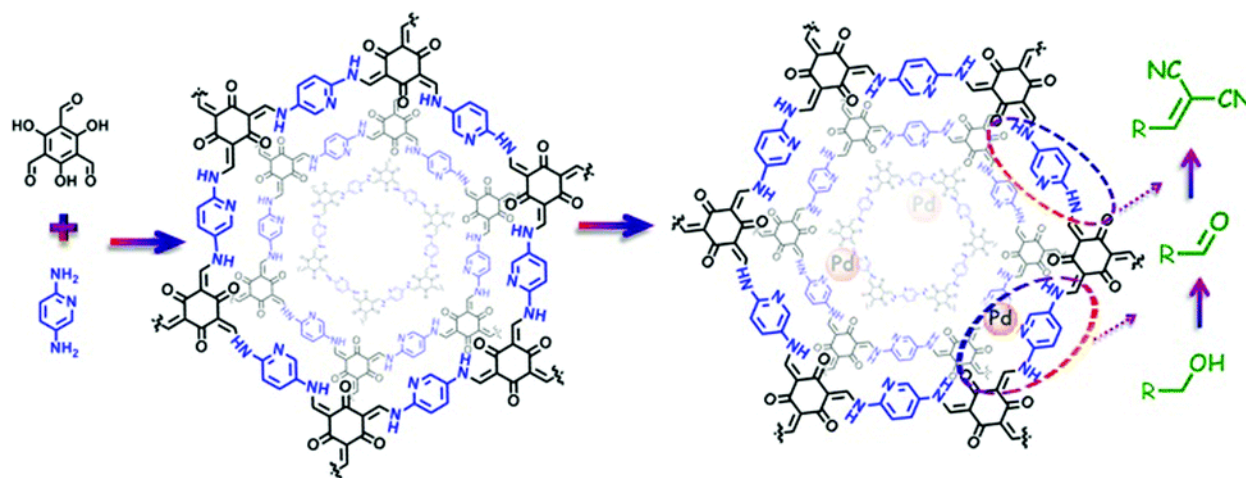


Figure 8. Pd-based pore surface engineering of COF-TpPa-Py for one-pot cascade catalysis.

Reproduced with permission from ref. 111. (Copyright © 2017, The Royal Society of Chemistry)

The pendant functional group in the well-defined pore channel of frameworks undergo conversion using established organic chemistry especially addition and substitution reactions which in turn, overcome with tedious chemical synthetic and purification procedure. Click reaction is predominantly used to introduce different functional groups such as ester, alcohols, thiols and others. Jiang research group report first ever example of copper catalyzed azide-alkyne cycloaddition click (CuAAC) reaction⁷⁷, 2D mesoporous boronate ester-linked COF-5 with uniformly distributed pendant azide functionalities at the walls of hexagonal skeleton used for pore surface engineering via click reaction with range of substituted alkynes to form five membered substituted frameworks. Notably, the percentage of azide moieties can be altered by varying the stoichiometric ratio of three components in a system. Same research group widened the possibility of this strategy by condensation of hydroxyl functionalized Zn-phthalocyanine, azide

functionalized 1,4-benzenediboronic acid and 1,4-benzenediboronic acid. The framework underwent pore surface engineering using CuAAC to covalently bound electron-acceptor [60] fullerene moieties, thereby acts as photoenergy conversion¹¹⁶. CuAAC reaction is relatively difficult to execute in B-O linked frameworks but, imine linked frameworks in comparison are more prone to similar fashion of pore surface engineering. Jiang research group synthesized alkyne functionalized COFs by condensation of porphyrin / Ni-porphyrin with 2,5-bis(2-propynyloxy)terephthalaldehyde and 2,5-dihydroxy terephthalaldehyde. By virtue of CuAAC reaction, the electronic environment of -OH, -COOH, -COOMe, -NH₂ functionalized frameworks¹¹⁷ drastically changed, furthermore, the same group also highlighted the assimilation of polyradical in the pore channel to induce redox nature in the framework, which is difficult to execute via *de novo* synthesis¹¹⁸. To extend this study, C₃-symmetric 1,3,5-tris(4-aminophenyl) benzene organic scaffold with same aldehyde monomers employed in different afford [HC≡C]_x-TBP-DMTP-COFs. Pore surface engineering via CuAAC using differently functionalized azides including chiral pyrrolidine, thiol, uracil, 2,2,6,6-tetramethyl-1-piperidinyloxy (TEMPO) radical form corresponding modified frameworks (Figure 9), in particular, chiral framework serve as catalyst for asymmetric Michael reactions with high activity and enantioselectivity¹¹⁹. Nucleobase-modified framework exhibited selective recognition of complementary nucleobase in aqueous solution¹²⁰, in addition, thiol engineered COF showed selective capture of Hg²⁺ from 10 mg L⁻¹ to 1.5 mg L⁻¹ within few minutes, well below the acceptable limit for drinking water (2 mg L⁻¹)¹²¹.

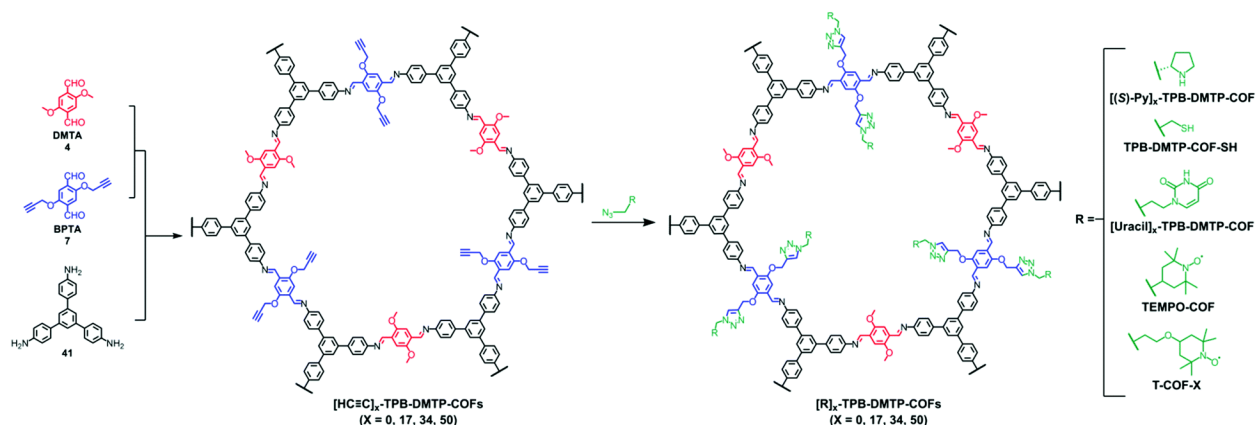


Figure 9. Pore surface engineering of [HC≡C]_x-TPB-DMTP-COFs via click chemistry. Reprinted with permission from ref. 141. (Copyright © 2019, Royal Society of Chemistry)

Sticking to the focal role of COFs as robust platform for environmental remediation, Dichtel research group reported thiol-ene free radical addition reaction inside pore channel of COFs¹²². Our research group reported 2D COF-V framework constructed by dynamic imine condensation of 1,3,5-tris(4-aminophenyl) benzene and 2,5-divinylterephthalaldehyde, followed by pore surface engineering via thiol-ene “click” reaction using 1,2-ethanedithiol and AIBN with complete retention of crystallinity and porosity. Due to the higher degree of vinyl group participation, nearly 90% of click chemistry led to uniform distribution of binding thiol functionalities in COF-S-SH for mercury removal. The high mercury uptake with 1350 mg g⁻¹ and 863 mg g⁻¹ for Hg²⁺ and Hg⁰ respectively in aqueous solution. Fascinatingly, COF-S-SH exhibited diffusion coefficient ($K_d = 2.3 \times 10^9$ mL g⁻¹) with high mercury uptake record from 5 ppm to 0.1 ppb which is far less than acceptable limit of drinking water (2 ppb). The flexible binding arms electronically and sterically adopt favorable conformation to exclusively interact with mercury via two sulphur atoms as confirmed by EXAFS, XPS, Raman spectra and other analytical techniques¹²³. In 2018, our research group highlighted integration of superwettability using same

click reactions by grafting fluorinated compounds. The highly efficient absorption of oil along with various toxic solvents such as nitrobenzene with an uptake capacity up to 142 times of its mass¹²⁴. This study addresses the growing ecological and environmental concerns with oil spills took place in the world and materials such as activated carbon and zeolite proven to be relatively ineffective. COFs as platform for environmental remediation studies extended to uranium removal from sea water. Amidoxime moieties in organic scaffold to construct framework via *de novo* synthesis is of profound challenge, our research group used cyano functionalized β -ketoenamine COF-TpDb prepared by condensation of triformylphloroglucinol and 2-cyano-1,4-phenylenediamine. Cyano group uniformly distributed in the pore channel of framework undergo pore surface engineering via conversion of cyano functionalities to amidoxime (COF-TpDb-AO) by reaction with hydroxylamine in methanol (Figure 10). COF-TpDb-AO used as uranium scavenger reduce uranium contaminated water samples from 1 ppm to 0.1 ppb in short time, furthermore, we also highlighted selectivity, adsorption affinities, capacities and kinetics¹²⁵. In addition to this conversion, cyano group partially hydrolyze to amide in basic medium¹²⁶ and completely hydrolyze to carboxylic acid or reduced to amine as highlighted by Yan, Valtchev and co-workers¹²⁷. Apart from amidoxime functionalities, introduction of $-NH_2$ moieties is demanding too but, amine being binding units with formyl to construct imine-linked COFs therefore, possibility of pendant $-NH_2$ in COFs is stiff via *de novo* fashion. Dichtel research group reported¹²⁸ pendant $-NH_2$ functionalized COF via pore surface engineering of (X% $[N_3]$ -COF) prepared by condensation of 1,3,5-tris(4-aminophenyl) benzene with appropriate ratio of azide-functionalized ethylene glycol terephthalaldehyde and terephthalaldehyde using PPh_3 in CH_3OH . The amine moieties in the pore channel of frameworks exhibited excellent crystallinity, surface area of over $1000\text{ m}^2\text{g}^{-1}$ and fast uptake of GenX. Chiral framework reported by Wang research group prepared

by condensation of chiral *N*-Boc-protected building block with 1,3,5-triformylbenzene or triformylphloroglucinol undergo cleavage of BOC under acidic, basic or heating condition and serve as organocatalysts for asymmetric aldol reaction¹²⁹.

Not all functionalities are difficult to uniformly decorated and modified in the frameworks, one of those functionalities is -OH. Jiang research group reported COFs bestow with uniform distribution of hydroxyl functionalities by reaction of 2,5-DHTA with porphyrin scaffold. The [OH]_{x%}-H₂P-COFs (X = 25, 50, 75, 100) on reaction with succinic anhydride undergoes ring opening reaction to form pendant carboxylic groups¹³⁰. Moreover, Gao research group reported modification by using acylation reaction in presence of range of substituted acyl chloride such as azobenzene and stilbene¹³¹. Same research group employed hydroxyl fu-

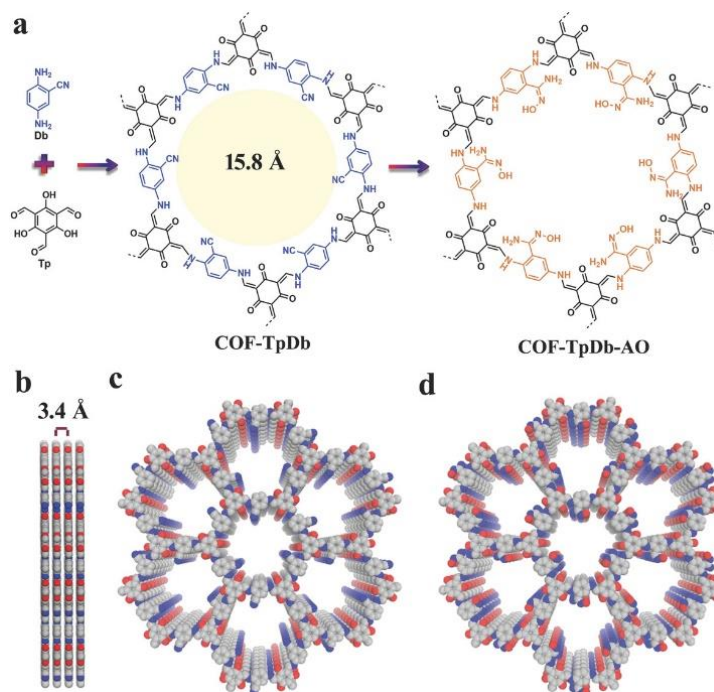


Figure 10. COF-TpDb synthesis using dynamic imine linkage and corresponding pore surface engineering to amidoxime group (COF-TpDb-AO); b,c,d.) Graphic view of the eclipsed stacking

structure of pristine and modified frameworks. Reproduced with permission from ref. 125.

(Copyright © 2018, Wiley-VCH Verlag GmbH & Co. KGaA, Weinheim)

nctionalized imine linked frameworks [HO]_{x%}-Py-COFs prepared by condensation of PyTTA and 2,5-dihydroxyterephthalaldehyde and terephthalaldehyde in different ratio for pore surface engineering via Williamson synthesis reaction using (2-bromoethyl) triethylammonium bromide. The modified frameworks [Et₄NBr]_{x%}-Py-COFs] (X = 25, 50) catalyzed *N*-formylation of amines with CO₂ and PhSiH₃, more importantly, a step towards metal-free catalysis (green catalysis)¹³². Same catalytic reaction was also highlighted by zwitterionic frameworks prepared by surface functionalization of hydroxyl decorated frameworks using Williamson synthesis reaction by treatment with 2-((3-bromopropyl) dimethylammonio) acetate¹³³. Last year, Fang, Valtchev research group synthesized hydroxyl-functionalized 3D COF by condensation of tetra(4-formylphenyl) methane and 3,3'-dihydroxybenzidine. The uniformly decorated hydroxyl groups on reaction with succinic anhydride afford pendant acyl carboxyl group, which in turn, showed selective binding of Nd³⁺ over Sr²⁺ and Fe³⁺ as proven by XPS, ¹³C NMR with excellent recyclability¹³⁴. Medina, Bein and co-workers also highlighted the reactivity of hydroxyl functionalized COFs by fluorescent dyes under normal reaction condition with no hindrance to crystallinity¹³⁵ along with facile approach to reduce nitro functionalized COFs to amine moieties via pore surface engineering in presence of SnCl₂.2H₂O which on further treatment with acetic anhydride under aminolysis to form amide functionalized COFs¹³⁶.

Zhou research group used 2,2'-bipyridine-based TpBpy framework reported by Banerjee *et. al.*¹³⁷ to study Ni-based pore surface engineering using Ni(ClO₄)₂ as ion sources to form Ni-TpBpy. PXRD, XPS, FT-IR, UV-Vis, SEM, HAADF-STEM affirm the successful immobilization

of nickel on framework, furthermore, the surface area and pore volume decrease from $973 \text{ m}^2\text{g}^{-1}$, $0.6 \text{ cm}^3\text{g}^{-1}$ to $580 \text{ m}^2\text{g}^{-1}$, $0.4 \text{ cm}^3\text{g}^{-1}$ albeit, increase in CO_2 uptake for Ni-TpBpy affirm the strong Lewis acid-base interaction between the nickel ions and carbon dioxide molecules. Extracting the knowledge of catalytic properties Ni-linker complexes for CO_2 reduction, the group investigated the photocatalytic CO_2 conversion activity of Ni-TpBpy using $[\text{Ru}(\text{bpy})_3]\text{Cl}_2$ (bpy = 2,2'-bipyridine) as photosensitizer and triethanolamine (TEAO) as an electro donor. The evolutions of CO and H_2 from Ni-TpBpy catalytic system in 5 h with CO and H_2 amounts are 4057 and $170 \mu\text{molg}^{-1}$ respectively with turn over number for CO evolution is 13.62 after 5 hours irradiation. Moreover, control experiments were also performed to point out the key factors for CO_2 to CO conversion and also investigate the negligible impact of TpBpy, Co^{2+} , Fe^{3+} , Zn^{2+} and Mn^{2+} immobilized frameworks. To gain mechanistic insight into the photocatalytic reduction of CO_2 by using Ni-TpBpy, cyclic voltammetry and DFT calculations were also reported¹³⁸.

TTB-COF solvothermally synthesized by imine condensation of 2,5-bis(2-(ethylthio)ethoxy)terephthalohydrazide (BETH) and 1,3,5-triformylbenzene (TFB) verified structurally by means of FT-IR, ^{13}C -NMR, UV-Vis with low surface area / pore volume and crystallinity is analyzed by PXRD. Due to the uniform distribution of pendant functionalities, Au ions captured with over 98% within few minutes ($K_{\text{SV}} = 4.46 \times 10^5 \text{ M}^{-1}$). In a mixture solution of Au^{3+} , Fe^{3+} , Ni^{2+} , Co^{2+} , Zn^{2+} and Cd^{2+} at 10 ppm concentration exhibited high capture of Au ions verified by XPS, EDX via SEM showed uniform distribution of gold within the framework¹³⁹. Recently, our group highlighted immobilization of iridium by reaction of Py-2,2'-BPyPh COF and $[\text{Ir}(\text{OMe})(1,5\text{-cod})]_2$ at room temperature under inert atmosphere. The iridium decorated framework, $(\text{Ir}_{\text{cod}}(\text{I})@\text{Py-2,2-BPyPh COF})$, exhibited complete retention of crystallinity, high thermal and chemical stability and surface areas of $859 \text{ m}^2\text{g}^{-1}$. The iridium docking was further

confirmed by ^{13}C MAS NMR, XPS, EPR, SEM-EDS and investigated as heterogeneous catalyst for C–H borylation reaction using bis(pinacolato)diboron (B_2pin_2) as borylating agent¹⁴⁰. Mechanistically, Ir(I) on reaction with B_2pin_2 converted to Ir(III) followed by oxidation addition to arene to form Ir(V), which in turn, undergoes reductive elimination to form organoboron product along with regeneration of catalyst.

Metal-free COFs functionalization

Pore surface engineering via metal coordination is widely studied and similar principle can also extend to backbone modifications using established organic chemistry and influence of non-covalent interactions to address various applications. The fundamental properties attached to the symmetric monomer and dynamic linkages present in the frameworks impart COFs with essential properties such as pore size, pore design, crystallinity and many more, which can be engineered to achieve desired outcomes¹⁴¹. Yaghi and co-workers reported conversion of imine linkage in COFs to amide functionalities in presence of sodium chlorite, 2-methyl-2-butene, acetic acid in dioxane. The conversion and progress of reaction was followed by Fourier-transform infrared spectroscopy (FT-IR), ^{13}C cross-polarization magic angle spinning (CP-MAS) NMR spectroscopy and PXRD measurements¹⁴². Cui research group further extend this idea from 2D COFs to 3D COFs under the same reaction condition¹⁴³. The difference between the stability of imine and amide framework is prominent in both acidic and basic media, amide frameworks $\{(R,R)\text{-CCOF6}\}$ in comparison to imine framework $\{(R,R)\text{-CCOF5}\}$ exhibited superior activity as chiral stationary phase for high performance liquid chromatography for enantioseparation of racemic alcohol. Feng, Wang and co-workers highlighted peculiar behavior of hydroxyl functionalized crystalline DABH-TFP-COFs prepared by the condensation of 2,5-diamino-1,4-dihydroxybenzene dihydrochloride (DABH) and

1,3,5-triformylphloroglucinol (TFP). The framework subjected to pore surface engineering to form benzoquinone functionalized DABQ-TFP-COF by oxidation with O_2 and NEt_3 as exhibited by FT-IR and other physiochemical analysis with faster kinetics of lithium storage. Interestingly, the vice versa, condensation of 1,3,5-triformylphloroglucinol and 2,5-diamino-1,4-benzoquinone (DABQ) does not give same result, instead form amorphous material (Figure 11)¹⁴⁴.

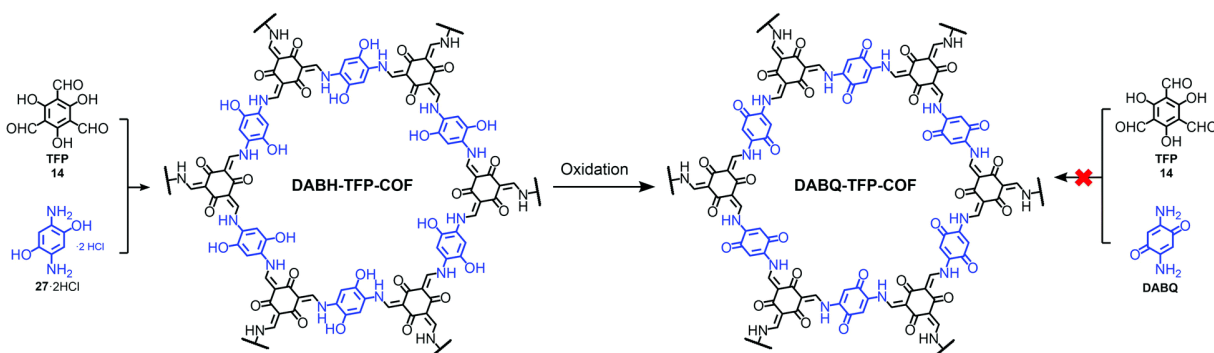


Figure 11. Chemical conversion of DABH-TFP-COF to DABQ-TFP-COF via oxidation of hydroquinone units. Adapted with permission from ref. 141. (Copyright © 2019, Royal Society of Chemistry)

Last year, Lotsch research group under harsh reaction condition exhibited sulphur abetted conversion of imine linked framework to thiazole-based framework via two successive pore surface engineering steps (Figure 12). Firstly, at elevated temperature ($155\text{ }^{\circ}\text{C}$) less viscous sulphur mix with framework and secondly, increase the temperature up to $350\text{ }^{\circ}\text{C}$ led to imine to thioamide and finally oxidized to thiazole ring conversion. These sequential conversions inside the pore channel was confirmed by PXRD, ^{13}C and ^{15}N solid state NMR spectroscopy¹⁴⁵. To a certain extent, similar imine conversion under relatively moderate condition was achieved by pore surface engineering of polarized imine-linked COF with substituted alkyne in presence of $BF_3 \cdot OEt_2$. Liu research group highlighted this cyclization by kinetically adjusting the imine bond with substituted

acetylene via aza-Diels-Alder cycloaddition reactions. Notably, the quinoline-based framework is among one of the robust frameworks reported COFs till today, withstand at severe reaction condition such as 12 M HCl, 14 M NaOH, KMnO_4 , NaBH_4 ¹⁴⁶.

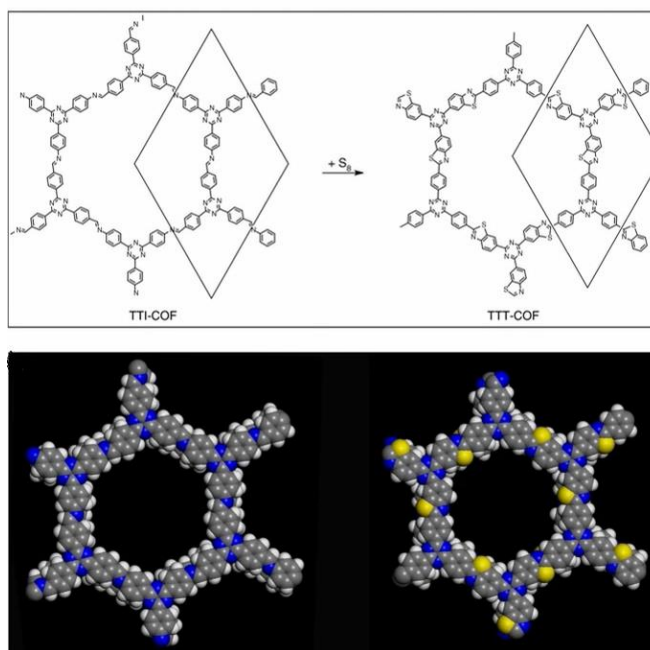


Figure 12. Conversion of imine-linked TTI-COF to thiazole TTT-COF using S_8 with space filling model of one pore. Reprinted with permission from ref. 145. (Copyright © 2018, Nature Publishing Group)

Recently, Xu, Chen and co-workers used vinyl functionalized COF-V to immobilized sulphur within the pore channel via inverse vulcanization strategy¹⁴⁷. After grinding the framework with elemental S_8 , the mixture heated at elevated temperature (155 °C) under inert atmosphere to immobilize molten sulphur and to ensure complete polymerization followed by heating at 200 °C. S-COF-V used as cathode for Li-S battery highlighting initial capacity of 1400 mA h g^{-1} and moderately declined to 959 mA h g^{-1} after 100 catalytic cycle, to the best of our knowledge this is one of the best performances of the hybrid porous materials. Zhang, Awaga and co-workers¹⁴⁸

used inverse vulcanization strategy in alkyne functionalized frameworks instead of vinyl analogue. The hybrid material formed acts as cathode for rechargeable lithium organic batteries with a capacity of 425 mA h g⁻¹. Same research group used aromatic nucleophilic substitution (S_NAr) strategy via *S*-arylation for covalent linkage to sulphur in frameworks backbone. COF-F synthesized by condensation of 1,3,5-tris(4-aminophenyl) triazine and 2,3,5,6-terephthalaldehyde undergo pore surface engineering in two steps, firstly, S₈ and framework in 3:1 weight ratio heated at 160 °C for 15 hours to immobilize sulphur into frameworks pore channel, secondly, to assist S_NAr reaction, the temperature increases to 350 °C for another 15 hours. COF-F-S exhibited high porosity, crystallinity with 60 wt% sulphur loading serve as cathode material for lithium-sulphur batteries¹⁴⁹.

COFs pore surface engineering achieved by backbone modification or metal immobilization is not the only ways to tune the chemically and sterically environment of pore channel. But, also by drawing advantage of bond dissociation and bond association under thermodynamic control. This way of conversion along with metal replacement extensively reported in MOFs. Zhao research group used TP-COF-BZ prepared by condensation of 1,3,5-triformylbenzene and benzidine underwent COF to COF transformation by monomer exchange using *p*-phenylenediamine to form TP-COF-DAB¹⁵⁰. To drive the equilibrium forward, *p*-phenylenediamine added in higher concentration to ensure complete conversion in short period of time (4 h). Notably, in comparison to TP-COF-DAB, TP-COF-BZ exhibited lower thermal stability and crystallinity. By this pivotal strategy, the frameworks crystallinity can be substantially improved, Horike research group employed two imine-linked COFs prepared by dynamic imine linkage between benzene-1,3,5-tricarbaldehyde with 1,4-diaminobenzene and 1,4-diaminonaphthalene. The author looks at both sides for building block exchange, firstly, benzene-

based COF reacted with different equivalents of 1,4-diaminonaphthalene led to replacement of 1,4-diaminobenzene with 1,4-diaminonaphthalene in different ratio. Interestingly, the modified framework exhibited improved crystallinity, two-fold increment in surface area with similar morphology and conversion further confirmed by high-angle annular dark-field scanning transmission electron spectroscopy (HAADF-STEM). Vice versa study of substituting monomer in naphthalene-based COF with 1,4-diaminobenzene under same reaction condition is enormously difficult due to robust π - π interaction (Figure 13). It is worth pointing that electronic and steric environment of building block is not the only factor to undergo monomer exchange but, also the chemical and thermal stability of framework draws from non-covalent interactions¹⁵¹. The introduction of various functionalities such as amino groups in COFs via *de novo* synthesis is of profound challenge in front of research community however, pore surface engineering addresses such pivotal challenges without any hindrance to frameworks crystallinity and morphology. With this approach in mind, Yan research group used two frameworks prepared by condensation of 1,3,5-tris(4-formyl) triazine with 1,4-phenylenediamine and benzidine. To impart $-\text{NH}_2$ functionalities uniformly in frameworks, the pristine COFs reacted with amino substituted phenylenediamine / benzidine at 40 °C for 72 hours¹⁵². Notably, the geometry of monomer may be of vital importance as reflected in reaction condition, which is far moderate than traditional way of constructing COFs.

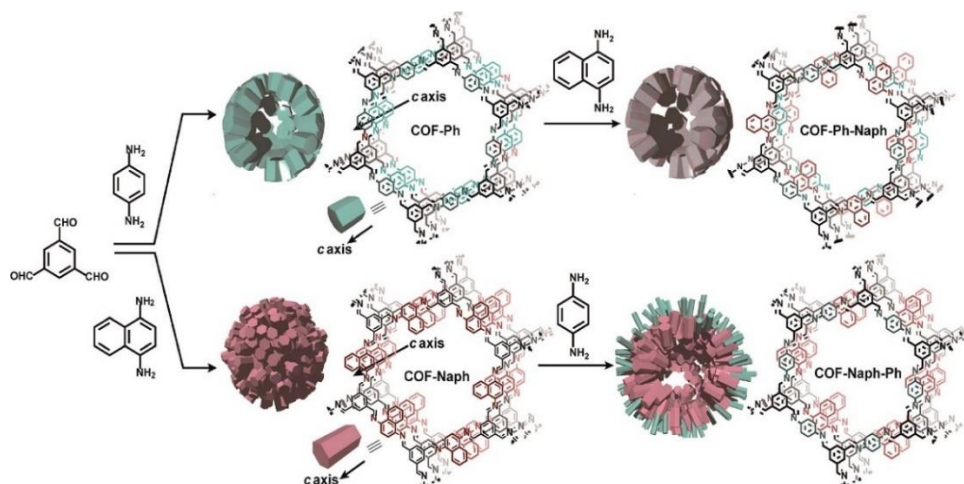


Figure 13. COF-Ph, COF-Naph and COF-Naph-Ph synthesis via pre and postsynthetic process.

Reproduced with permission from ref. 151. (Copyright © 2018, American Chemical Society)

Zhao *et al* reported approach to induce amino functionalities at high reaction rate probably due to the electronic environment of monomer. Building block exchange strategy positively influence the stability of frameworks via cyclization, imine-linked IL-COF-1 synthesized by condensation of 1,4-phenylenediamine and 1,3,6,8-tetrakis(4-formylphenyl) pyrene undergoes linker exchange using 2,5-diaminobenzene-1,4-dithiol dihydrochloride and 2,5-diaminohydroquinone dihydrochloride followed by oxidation to form stable oxazole-containing COF-921 and azole-containing LZU 192 respectively¹⁵³. Recently, Dichtel research group synthesized β -ketoenamine-linked frameworks by building block exchange of 1,3,5-triformylbenzene with triformylphloroglucinol, as expected, the framework showed excellent crystallinity, stability and higher surface area¹⁵⁴.

APPLICATIONS: The high degree of crystallinity helps in establishing structure-property relationship by offering numerous innovative ways to uniformly position range of moieties

including different functional groups. The sole presence of light elements (B, C, N, O) makes framework less dense (COF-108 = 0.17 g cm^{-3}) in comparison to other porous crystalline solids. In addition, high surface areas and pore volume along with uniform and periodic accessible pores added remarkable advantage to COFs (COF-103 = $4210 \text{ m}^2 \text{ g}^{-1}$ and $1.66 \text{ m}^3 \text{ g}^{-1}$)^{38,73}. The utilization of hydrogen bonding, Michael addition-elimination route in addition to dynamic covalent linkage keep COFs resistance to thermal and chemical environment¹⁵⁵. This high resistance towards hydrolysis, oxidation / reduction environments and wide range of pHs hardly evident by other porous materials open structural modularity via pore surface engineering thereby, serve as an attractive and ideal platform for different applications.

BIOMEDICAL: Yan and co-workers designed 3D polyimide frameworks (PI-COF-4 and PI-COF-5)¹⁵⁶ by imidization between tetrahedral 1,3,5,7-tetraaminoadamantane (TAA) or tetra(4-aminophenyl) methane (TAPM) and pyromellitic dianhydride (PMDA) with pore size of 1.3 nm and 1.0 nm. Ibuprofen ($5 \text{ \AA} \times 10 \text{ \AA}$), a widely used drug with short biological half-life ($t_{1/2} = 2 \text{ h}$) trapped inside the pore channel of PI-COF-4 and PI-COF-5 exhibiting excellent release control. For both frameworks, the slow drug delivery was observed (6 days) and reached to 95% in comparison to initial loading. Notably, relatively lower release rate was examined for PI-COF-5 due to less pore size (1.0 nm) and interpenetrated structure, moreover, the same frameworks showed similar level of delivery rate with captopril and caffeine. In vivo biocompatibility and cytotoxicity of COFs have been less explored as compared to in vitro, Zhao research group¹⁵⁷ used two imine linked frameworks, namely PI-2-COF and PI-3-COF for cell experiments. Both PI-2-COF and PI-3-COF showed high drug loading capacity for ibuprofen, captopril and 5-fluorouracil (5-FU) with release out in 3 days.

To substantially increase the biocompatibility, Banerjee research group reported¹⁵⁸ salt mediated scalable synthesis of TpAPH and TpASH frameworks followed by sequential pore surface engineering to form required hybrid material (TpASH-FA). In specific, essential sites required for cellular targeting agents was achieved by modification of hydroxyl functionalized framework through ring-opening of glycidol. The continuous release of 5-FU from functionalized frameworks killed cancer cells via apoptosis. The interaction between COFs and immobilized drug translates into better control of drug delivery. Lotsch and co-workers¹⁵⁹ constructed TTI-COF by condensation of 1,3,5-tris(4-formyl) triazine and 1,3,5-tris(4-amino) triazine to study quercetin (3,3,4,5,7-pentahydroxyflavone) behavior to human breast carcinoma MDA-MB-231 cells. Molecular dynamics simulations studies show that drug was interacted with pore walls via C—H— π and H-bonding interactions. Quercetin decompose slowly over a wide temperature range, therefore, TGA analysis failed to calculate the loading amount. Unfortunately, the drug prone to oxidation and difficult to dissolve in buffer inhibits in vitro drug release study. However, in comparison to pristine framework, drug-loaded framework showed moderate activity towards MDA-MB-231 cells, this study even after few limitations unambiguously explained material synthesis and role of framework as drug delivery vehicle. Apart from COFs role as drug delivery carrier, Bhaumik research group highlighted¹⁶⁰ the role of functional COF as anticancer agents. EDTFP-1 COF prepared by condensation reaction of 1,3,5-triformylphloroglucinol and 4,4'-ethylenedianiline under inert atmosphere exhibiting the acceleration in the ROS generation due to phloroglucinol derivatives led to apoptosis of cancer cells like HCT 116, HepG2, A549 and MIA-Paca2 (Figure 14). Enzymes activity often suppress due to the deactivation at certain temperature and pH range. This hindrance can be diminished by coupling the enzyme chemistry to porous materials chemistry which primarily protect from deactivation and also provide a window of

stability and recyclability. Banerjee and co-workers first reported COFs for enzyme encapsulation by using mesoporous nature imine linked framework synthesized by condensation of 2,5-dihydroxyterephthaldehyde and 1,3,5-tris(4-aminophenyl) benzene exhibited excellent crystallinity with BET surface area and pore size of $1480 \text{ m}^2\text{g}^{-1}$ and 3.7 nm respectively. Trypsin (hydrodynamic size = 3.8 nm) immobilization was confirmed by confocal laser scanning microscopy and revealed moderate activity (60% of free enzyme) was retained in the hydrolysis of *N*-benzoyl-L-arginine-4-nitroanilide to 4-nitroaniline¹⁶¹. Our group in collaboration with Zhang and Chen research group highlighted framework with pendant carboxylic groups which on subsequent reaction with *N*-hydroxysuccinimide and amine linked biomolecules such as peptide afford biomolecules decorated pore channel COF (biomolecules \square COFs) serve as chiral stationary phase in both reverse and normal phase high-performance liquid chromatography¹⁶². Furthermore, we also investigate the enzymatic performance of lipase PS encapsulated in various mesoporous materials for kinetic resolution of racemic 1-phenylethanol with vinyl acetate, more importantly, higher catalytic activity was observed for immobilized porous materials in comparison to free enzyme. We also studied the tunability of hydrophobic or hydrophilic environment inside pore channel of COFs by exposure of phenolic COF in basic medium (aq. NaOH) to form $-\text{ONa}$ functionalized COF which in comparison to isorecticular COF with $-\text{OMe}$ moieties showed significantly lower uptake of lipase¹⁶³.

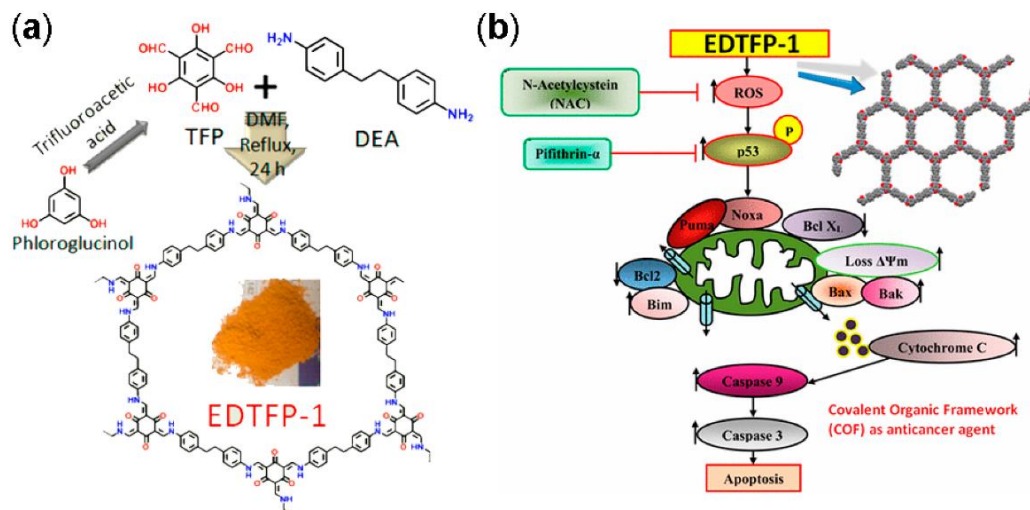


Figure 14. a.) Synthesis of EDTFP-1 from TFP and DEA and b.) It's induced apoptotic pathway.

Adapted with permission from ref. 160. (Copyright © 2017, American Chemical Society)

Photothermal therapy (PTT) was studied by Guo research group by deposition of imine-linked framework on the surface of Fe_3O_4 nanoclusters. The resulted $\text{Fe}_3\text{O}_4@\text{COF}$ not only elevates the temperature by 25 °C but, also affect photothermal conversion efficiency by 21.5%, which is comparable to some reported photosensitizer such as gold nano rods¹⁶⁴. Moreover, Xie and co-workers¹⁶⁵ grew imine-based porphyrin COF on the surface of amine functionalized MOF with average size of 176 nm, hybrid UNM material produce singlet oxygen and showed significant toxicity for HepG2 and HeLa upon irradiation using confocal laser scanning microscopy however, no activity was observed without light. Antimicrobial application of COFs is very sporadic in literature, Banerjee research group construct self-exfoliated ionic covalent organic nanosheets by using guanidinium halide and 1,3,5-triformylphloroglucinol. The guanidinium moieties formed hydrogen bond with phosphate anions whereas, positively charge CONs breaks negatively charged

phospholipid bilayer of bacteria. Antibacterial study indicated that these nanosheets showed excellent antimicrobial activity against gram-positive and gram-negative bacterial¹⁶⁶.

CATALYSIS: The continuous and sustainable advancement in the field of heterogeneous catalysis comes from environmental and economic challenges. This can be achieved by developing new hybrid materials to improve catalytic efficacy, lower cost, reduce waste, recyclability and reusability. Within this context, the use of porous materials such as COFs with chemical / thermal stability, high surface area and great tunability along with characteristics from both molecular and heterogeneous level is pivotal. The regular pore channel in COFs provide well-defined coordination sites and environment for different catalytic centers without disturbing the crystallinity and morphology of frameworks. In this subsection, we will summarize *de novo* synthesized COFs as heterogeneous catalysis.

Yan research group synthesized¹⁶⁷ 3D BF COFs by condensation reaction of 1,3,5,7-tetraaminoadamantane (TAA) with 1,3,5-triformylbenzene (TFB) or triformylphloroglucinol (TFP). The extraordinary stability of frameworks with surface area and pore size of 730 m²g⁻¹, 0.83 nm and 680 m²g⁻¹, 0.81 nm for BF-COF-1 and BF-COF-2 respectively catalyze Knoevenagel condensation between range of substituted aldehydes with malononitrile exhibited excellent conversion and size selectivity, for instance, benzaldehyde converted to 95% condensation product whereas, *p*-tolualdehyde afford <5% product. Zhao research group used sulfonated decorated TFP-DABA COF as effective catalyst for fructose dehydrate to 5-hydroxymethylfurfural (HMF) into 100 % conversion with 97% yield¹⁶⁸. Yaghi research group

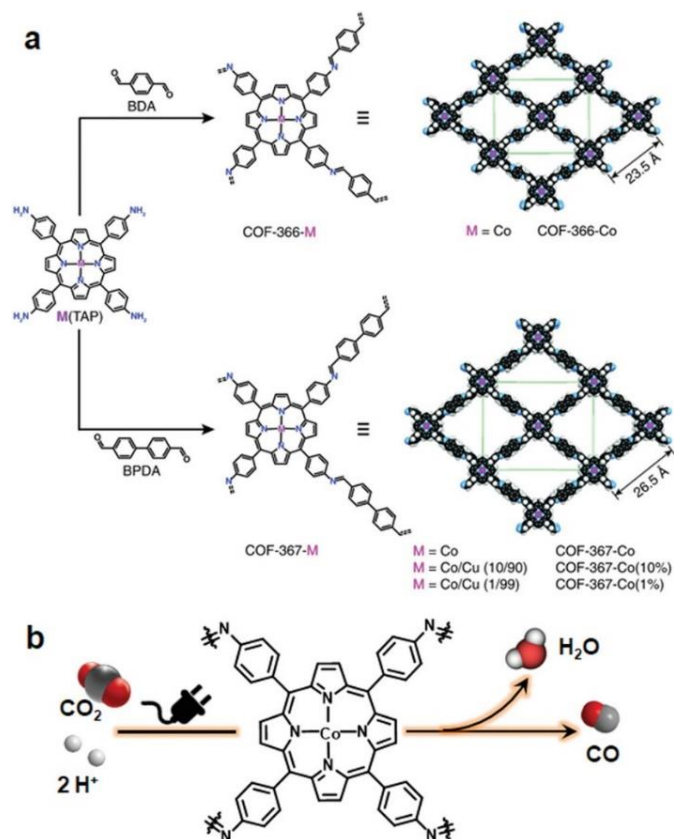


Figure 15. a.) Synthesis of metalloporphyrin-derived 2D COFs; b.) COF-366-Co based electrocatalytic reduction of CO₂ in water. Reprinted with permission from ref. 169. (Copyright

© 2015, American Association for the Advancement of Science)

reported COF-366-Co by Schiff base condensation of 5,10,15,20-tetrakis(4-aminophenyl) porphinato cobalt [Co(TAP)] and terephthalaldehyde for electrochemical reduction of CO₂ to CO. COF-366-Co showed 90% faraday efficiency for CO in 24 hours with turn over number (TON) of 34, 000, furthermore, Co(TAP) on condensation of 4,4'-biphenyldicarbaldehyde generates expanded pore size COF, thereby, positively influence the reduction with TON of 48, 000, substantially higher than COF-366-Co¹⁶⁹ (Figure 15). In addition, conversion of cycloaddition reaction between epoxide and CO₂ to form cyclic carbonate catalyzed by using imine-linked

hydroxyl decorated framework prepared by condensation of 2,3-dihydroxy terephthalaldehyde and 5,10,15,20-tetrakis(4-aminophenyl)-21H,23H-porphine¹⁷⁰.

Cui research group reported chiral COF by condensation of chiral tetraaryl-1,3-dioxolane-4,5-dimethanol (TADDOL) unit aldehyde scaffold and 4,4'-diaminodiphenylmethane. The chiral framework on treatment with $\text{Ti}(\text{OiPr})_4$ afford CCOF/Ti as an effective catalyst for asymmetric addition of diethyl zinc to aldehyde to form alcohol in high percentage yield, outperforming the corresponding homogeneous analogue (TADDOL/Ti)¹⁷¹. Same research group reported 3D framework by using same chiral monomer and tetra(4-anilyl) methane as high performance in liquid chromatographic enantioseparation¹⁴⁴. Shinde *et. al.* synthesized framework bearing weak acidic and basic sites by condensation reaction between 5,10,15,20-tetrakis(4-aminophenyl) porphyrin and 2,3-dihydroxyterephthalaldehyde as an effective catalyst for domino reaction. The uniformly distributed porphyrin and imine moieties served as weak basic sites whereas, catechol groups act as weak acid sites. Due to the presence of weakly basic and acidic sites at vertices and edges respectively in the framework serve as heterogeneous catalyst for cascade reaction of benzaldehydedimethylacetal and malononitrile in high yield¹⁷². Similar tandem reaction was also highlighted by 3D frameworks prepared by boroxine linkage between 1,3,5,7-tetraaminoadamantane and 4-formylphenylboronic acid / 2-fluoro-4-formylphenylboronic acid. Our own group in collaboration with Chen and Zhang research group synthesized squaramide-linked COF-SQ by reaction of 1,3,5-triformylbenzene and 3,4-bis((4-aminophenyl) amino)-cyclobut-3-ene-1,2-dione as organocatalyst for Michael addition under mild condition¹⁷³ (Figure 16).

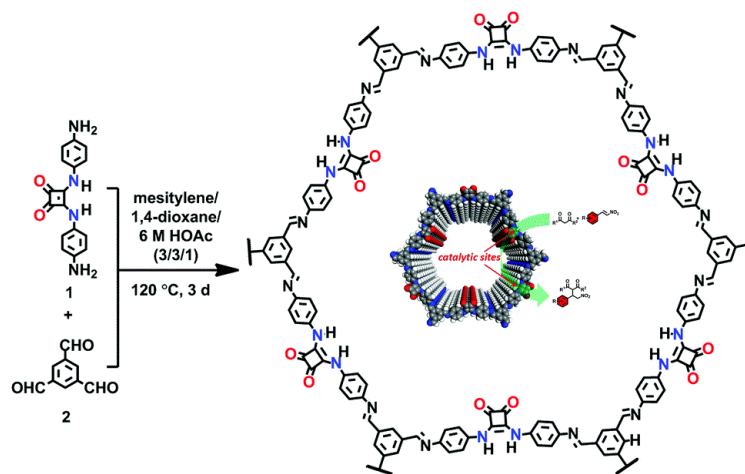


Figure 16. Synthesis of squaramide-linked organocatalyst COF-SQ. Reproduced with permission from ref. 173. (Copyright © 2019, Royal Society of Chemistry)

Lotsch research group reported COFs as an ideal platform for the construction of photoactive catalysts. The condensation reaction of hydrazine with triphenylarylaldehydes with core ring having varying ratio of nitrogen atoms (0-3) afford N_x -COFs (X = no. of nitrogen). The hydrogen evolution increases from 23, 90, 438 to 1703 $\mu\text{mol h}^{-1}$ with increase in nitrogen concentration of N_0 -COF, N_1 -COF, N_2 -COF and N_3 -COF respectively after 8 h¹⁷⁴. Bein and co-workers synthesized stable BDT-ETTA COF by condensation of 1,1',2,2'-tetra-*p*-aminophenylethylene (ETTA) and benzo[1,2-*b*:4,5-*b'*]-dithiophene-2,6-dicarboxaldehyde (BDT) as photoelectrode for photoelectrochemical water splitting in absence of sacrificial agent and cocatalyst¹⁷⁵. Furthermore, Banerjee and co-workers reported¹⁷⁶ amalgamation of photocatalytically active CdS nanoparticles in COF for visible-light-driven hydrogen production. The extensive π -conjugation in framework stabilized the nanoparticles and also prevents the recombination of electron and holes to facilitate charge transfer, in particular, 30% increment in H_2 evolution was observed for hybrid material in comparison to pristine framework.

ENVIRONMENTAL REMEDIATION: By virtue of high surface area, tailorable pore size and electronic environment, the potential of nuclear events and risks can be addressed using porous frameworks. To substantially increase the adsorptive capacity, kinetics and selectivity, a range of functionalities plays a pivotal role to battle pollutions. The nature and virtue of host molecules is of prime importance, for instance, amorphous host suffer from small pore size led to inaccessibility of grafting groups whereas, COFs presented with essential properties such as high pore size and others as summarized before led to the entrapment of heavy metal ions. More importantly, the presence of binding moieties uniformly distributed via *de novo* strategy or pore surface engineering in the COFs further brand COFs at forefront of this issues. There are range of binding moieties known to entrap uranium, as proof-of-concept, β -ketoenamines frameworks decorated with amidoxime functionalities used for sequestration of uranium far outperform amorphous solids in context of affinities, kinetics and absorption capacities¹²⁵. The decorated framework effectively removed uranium from water (408 mg g⁻¹) and diminish to 0.1 ppb which is far less than limits set up by U.S. Environmental Protection Agency.

Mercury is one of the important metal obstinate to public health problems. Explicitly, the selective capture of mercury to protect fresh water or any other contamination is a need of an hour. Wang research group reported hydrazine linked fluorescent LZU8 COF synthesized by condensation of 1,3,5-triformylbenzene and thioether-functionalized scaffold, thereby, decorating evenly and densely thioether functionalities in 1D pore channel for high affinity and selectivity towards mercury ions (Figure 17). LZU8 COF exhibited an uptake capacity of 300 mg g⁻¹ with a detection limit as low as 25 ppb with excellent recyclability¹⁷⁷. In addition, Jiang research group synthesized TAPB-BMTTPA-COF by condensation reaction of 2,5-bis(methylthio)terephthalaldehyde (BMTTPA) and 1,3,5-tris(4-aminophenyl) benzene (TAPB)

for mercury removal from aqueous solution. The thioether functionalized framework has abundantly decorated with sulphur functionalities led to uptake capacity to 734 mg g^{-1} , which is approximately 2.5 times higher than LZU8 COF¹⁷⁸. Qiu research group synthesized two novel 3D-ionic-COF-1 and 3D-ionic-COF-2 by condensation of tetrakis(4-formylphenyl) methane with diimidium bromide and ethidium bromide respectively¹⁷⁹. Both ionic frameworks exhibited high crystallinity, porosity, stability and potential for selective removal of permanganate. The observed kinetics with excellent recyclability supersedes signature materials such as PVBTAH-ZIF-8 and LDHs. Sticking to ionic frameworks, Trabolsi research group reported for the first time viologen-linked COF using Zincke reaction with excellent stability, porosity and controllable morphology. The condensation of 1,3,5-tris(4-aminophenyl) benzene and 1,1'-bis(2,4-dinitrophenyl)-[4,4'-bipyridine]-1,1'-diium dihydrochloride afford charged framework for iodine capture from both solution and vapors efficiently¹⁸⁰.

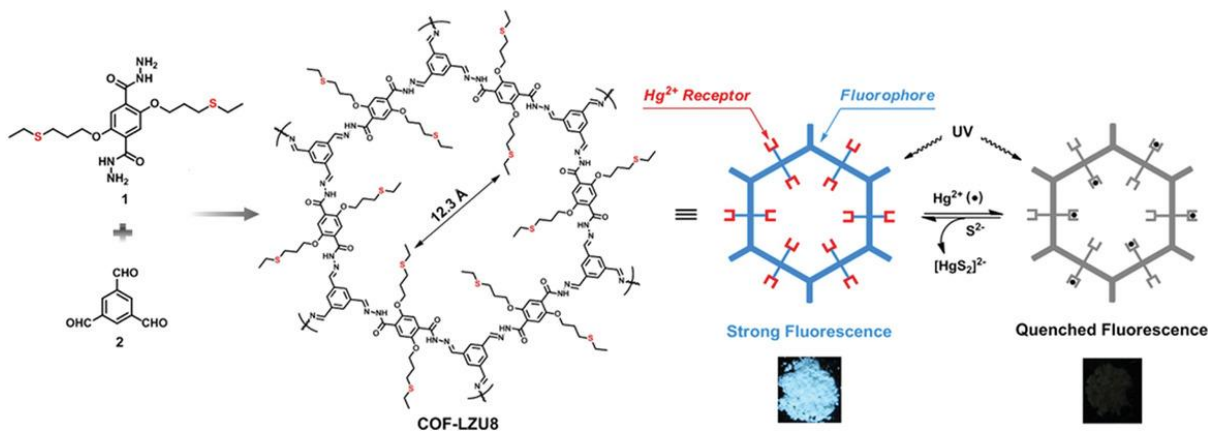


Figure 17. Synthesis of hydrazine-linked COF-LZU8 with thioether groups for removal of Hg^{2+} ions. Photographs of COF-LZU8 under a UV lamp ($\lambda = 365 \text{ nm}$) exhibited change in fluorescence after mercury adsorption. Adapted with permission from ref. 177. (Copyright © 2016, American Chemical Society)

Jiang research group reported cationic PyTTA-BFBI*m*-iCOF synthesized by dynamic imine linkage of PyTTA and ionic 5,6-bis(4-formylbenzyl)-1,3-dimethyl-benzimidazolium bromide (BFBI*m*) building block with BET surface area of 1532 m²g⁻¹. The decoration of benzimidazolium cations on either side of pores due to the reverse AA stacking mode led to excellent uptake capacity of negatively charged methyl orange dye (553 mg g⁻¹), which is highest among various porous materials probably due to high degree of electrostatic force of interactions. Furthermore, excellent CO₂ uptake capacity of 93 mg g⁻¹ and 177 mg g⁻¹ at 298 K and 273 K respectively was reported, significantly higher than neutral frameworks¹⁸¹. Loh research group synthesized salicylideneanilines-based COF (SA-COF) constructed by condensation reaction of 1,3,5-tris(4-aminophenyl) benzene and triformylphloroglucinol exhibited BET surface area and pore size of 1588 m²g⁻¹ and 1.43 nm respectively. Given the presence of reversible proton tautomerism and well-arranged pore channel, SA-COF explored as size-dependent organic pollutant separation. The binding affinity of framework with range of dye molecules declines with increase in molecular size and cannot entrap when guest size molecule exceeds to host pore size. Notably, the nature of dye and pH sensitivity also plays the role in changing pore environment and thereby selectivity in charged molecule separation¹⁸².

GAS STORAGE AND SEPARATION: In the post-carbon future, hydrogen will be an important alternative source of energy swiftly replacing nonrenewable source of energy such as coal or petrol. This green alternative has been one of the first applications explored using COFs, Yaghi research group reported¹⁸³ boroxine and boronic ester linked 2D and 3D COFs. It was found that medium sized 3D COF-102 and COF-103 at 77 K showed hydrogen uptake value of 72.4 mg g⁻¹ and 70.5 mg g⁻¹ respectively, which is substantially higher than 2D COF-1 (14.8 mg g⁻¹), COF-5

(35.8 mg g⁻¹), COF-6 (22.6 mg g⁻¹), COF-8 (35.0 mg g⁻¹) and COF-10 (39.2 mg g⁻¹). In addition to this, Qiu and co-workers highlighted imine- and boroxine-linked frameworks, denoted as, DL-COF-1 and DL-COF-2 synthesized by condensation of 1,3,5,7-tetraaminoadamantane with 4-formylphenylboronic acid and 2-fluoro-4-formylphenylboronic acid respectively. Both frameworks tested for H₂, CO₂ and CH₄ sorption behavior, DL-COF-1 showed 2.09 wt% H₂ sorption at 77 K, 26.7 wt% CO₂ sorption at 273 K, 2.57 wt% for CH₄ at ambient temperature whereas, DL-COF-2 exhibited 1.73 wt%, 21.8 wt%, 2.10 wt% sorption for H₂ at 77 K, CH₄ at 273 K, CO₂ at 273 K respectively¹⁸⁴. The improved hydrogen or carbon dioxide storage capacity of COFs further improved by spillover effect, Kalindi *et. al.* and Zhao group summarized theoretical studies of H₂ and CO₂ capture in a detailed review^{185, 186}.

Porous materials play profound role in industrial ammonia transportation, COFs synthesized by boroxine or boronate ester susceptible to Lewis acid and Lewis base interactions. The high density of boron atoms (Lewis acidic) in the framework trapped ammonia (Lewis base) through coordinate bond. Boroxine linked COF-10 prepared by dynamic linkage of hexahydroxytriphenylene and biphenyldiboronic acid showed ammonia uptake of 15 mol kg⁻¹ at 25 °C, which is substantially higher than signature materials such as Zeolites (9 mol kg⁻¹) and Amberlyst (11 mol kg⁻¹). Notably, at elevated temperature (200 °C) adsorbed ammonia evacuated and this adsorption/desorption cycling tested up to three runs without any significant variation in properties however, slight broadening and decrease in intensity observed in PXRD during subsequent cycles¹⁸⁷ (Figure 18). The role of open metal sites in ammonia uptake is profoundly studied in MOFs, so enriching and combining the advantages with chemically and thermally stable COFs is far beyond noticeable. Zhu and co-workers decorated¹¹² the wall of 2D imine linked framework with carboxyl functionalities under multicomponent condensation strategy. The role of

carboxyl moieties is abundantly evitable with nearly 50% increment (9.34 mmol g^{-1}) in comparison to pristine framework (6.85 mmol g^{-1}) at 298 K. The authors demonstrated binding of divalent metal ions such as calcium, strontium and manganese to carboxyl functionalities boost ammonia uptake. As expected, the ammonia uptake is substantially higher in all three metal incorporated materials, for instance, strontium integrated framework with an equilibrium ammonia uptake of $14.30 \text{ mmol g}^{-1}$. Zhu research group¹⁸⁸ construct microporous framework by condensation of 1,2,4,5-tetrahydroxybenzene and TBPM for selective C_2H_6 and C_2H_4 adsorption over CH_4 .

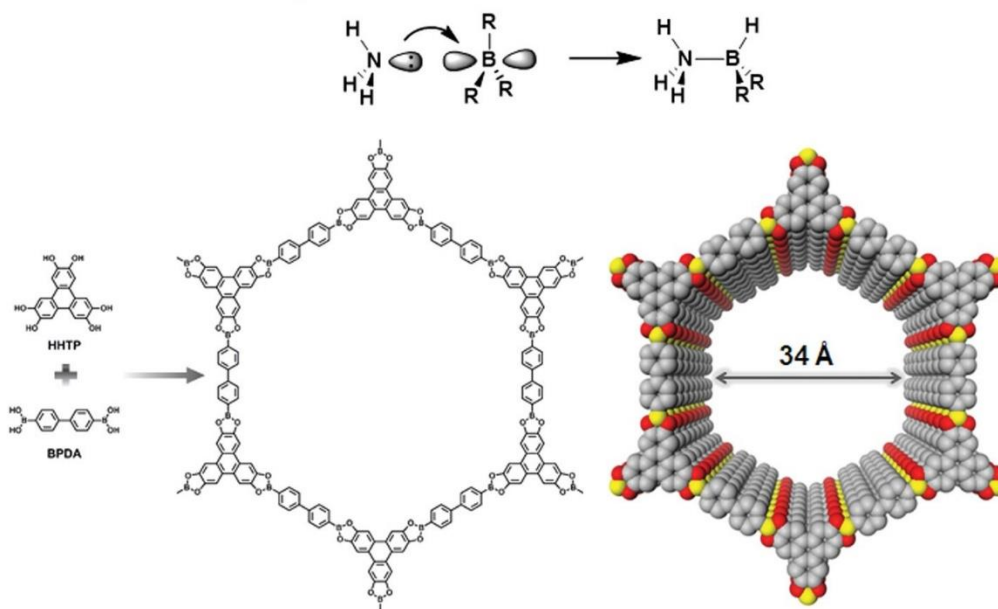


Figure 18. Lewis acid-base interaction between boron-ammonia; synthesis of COF-10 with eclipsed stacking structure. Reproduced with permission from ref. 187. (Copyright © 2010, Nature Publishing Group)

A negatively charged spiroborate framework constructed from trimethylborate and diol-functionalized macrocycle further introduced Li^+ counter ions for high H_2 and CH_4 storage capacities at 3.11 wt% and 4.62 wt% respectively. Furthermore, nitrogen rich nature frameworks

play favorable role in carbon dioxide adsorption. Cai *et. al.* reported¹⁸⁹ brick-wall COF prepared by condensation of PDA and 4,4',4''-(1H-benzo[d]imidazole-2,4,7-triyl) tribenzaldehyde with CO₂ capacity of 3.95 wt% and 40.43 wt% at 273 K and 195 K respectively. The central role of COFs in gas storage can be expanded to effective CO₂ capture and conversion to value-added chemicals which in turn, mitigate environmental concerns. In 2009, first report on CO₂ adsorption was reported, thereafter, Liu research group¹⁹⁰ synthesized azine-based framework (ACOF-1) by condensation of 1,3,5-triformylbenzene and hydrazine with pore size of 0.94 nm. The high percentage of nitrogen on the pore channel walls and high surface area of 1176 m²g⁻¹ exhibited high carbon dioxide uptake (177 mg g⁻¹), higher than various reported COFs. Jiang research group synthesized azide decorated framework (*x*%N₃-COF-5) by three components condensation under inert atmosphere followed by click reaction to form triazole-linked modified frameworks. The decorated frameworks were investigated for selective gas sorption of CO₂ over N₂ and found sixteen-fold increment in adsorption was observed from 25%PyTrz-COF-5 to 100%PyTrz-COF-5 as compared to pristine framework⁷⁷.

SENSING: The judicious choice of precursor units in constructing COFs with tunable pore size, electronic environment, functional moieties along with stacking interactions plays profound role in sensing under the shadow of non-covalent interactions. Dalapati *et. al.* synthesized stable azine-linked framework by condensation of 1,3,6,8-tetrakis(4-formylphenyl) pyrene and hydrazine. Due to the high percentage of fused benzene rings and hydrogen bonding synthons in framework serve as sensitive and selective sensor for 2,4,6-trinitrophenol⁴⁷. Similar principle was further extended for the selective fluorescence quenching of picric acid (75%, 20 ppm) using porous 3D-Py-COF

prepared by imine linkage between tetra(*p*-aminophenyl) methane and 1,3,6,8-tetrakis(4-formylphenyl) pyrene¹⁹¹.

Imide-linked thermal stable (>500 °C) PI framework¹⁹² constructed by condensation of 3,4,9,10-perylenetetracarboxylic dianhydride and tetra(4-aminophenyl) porphyrin showed high selectivity towards 2,4,6-trinitrophenol over the range of 0.5 to 10 μM with quenching constant and detection limit of $1 \times 10^{-7} \text{ M}^{-1}$ and 0.25 μM respectively. 3PD and 3'PD ketoenamine frameworks¹⁵⁵ constructed from Michael addition-elimination reactions exhibited quenching on treatment with various nitro- and peroxide explosives with a detection onset of $1 \times 10^6 \text{ M}$ for triacetone triperoxide probably originates from the oxidation of enamine units. Moreover, the sensing of various compounds including nitrobenzene, phenol and 2-nitrotoluene with effective fluorescence quenching was also reported by imine-linked TAT-COF-2 and TfpBDH framework synthesized by condensation of 2,7,12-triformyl-5,10,15-triethyltriindole with 2,7,12-triamino-5,10,15-triethyltriindole and pyromellitic-*N, N'*-bisaminoimide and 1,3,5-tris(4-formylphenyl) benzene respectively^{193,194}. The selective sensing studies does not restrict only up to nitro explosives but, also extended to the fluorescence quenching of ammonia. Boronic ester TPE-Ph framework⁸¹ synthesized by tetraphenylethylenetetraboronic acid and 1,2,4,5-tetrahydroxybenzene exhibited 30% fluorescence quenching upon addition of ammonia with k_q value of $6.3 \times 10^{14} \text{ M}^{-1} \text{ s}^{-1}$ and $1.4 \times 10^{14} \text{ M}^{-1} \text{ s}^{-1}$ in toluene and cyclohexane respectively. In addition to this, JLU-3 COF prepared by condensation of hydrazine and hydroxyl functionalized triformylbenzene, serve as chelating agents for transition metal ions. The strong fluorescence quenching observed for Cu^{2+} ions among other transition metal ions such as Co^{2+} , Fe^{3+} and Ni^{2+} ions with excellent recyclability is extraordinary¹⁹⁵, first fluorescent framework for selective and sensitive sensor of toxic metals.

Apart from metal ions and small explosive nitro molecules, DNA detection was highlighted by Zhang and co-workers synthesized [3+3] imine-linked framework¹⁹⁶ by condensation of tris(4-formylphenyl) amine and tris(4-aminophenyl) amine possess weak interlayer interaction due to flexible nature of precursor units. Due to these core properties, the framework readily exfoliated and exhibit excellent selective and sensitive of DNA with a limit of 20 pM (Figure 19). Moreover, Ajayaghosh research group reported fluorescent cationic ultrathin 2D sheets EB-TFP-iCONs by self-exfoliation of EB-TFP framework, given the electrostatic interactions between phosphate backbone of DNA and positively charged framework led to restacking as reflected in orange color emission. Notably, this hybrid sensor material shows remarkable in distinguishing dsDNA from single-stranded ssDNA¹⁹⁷.

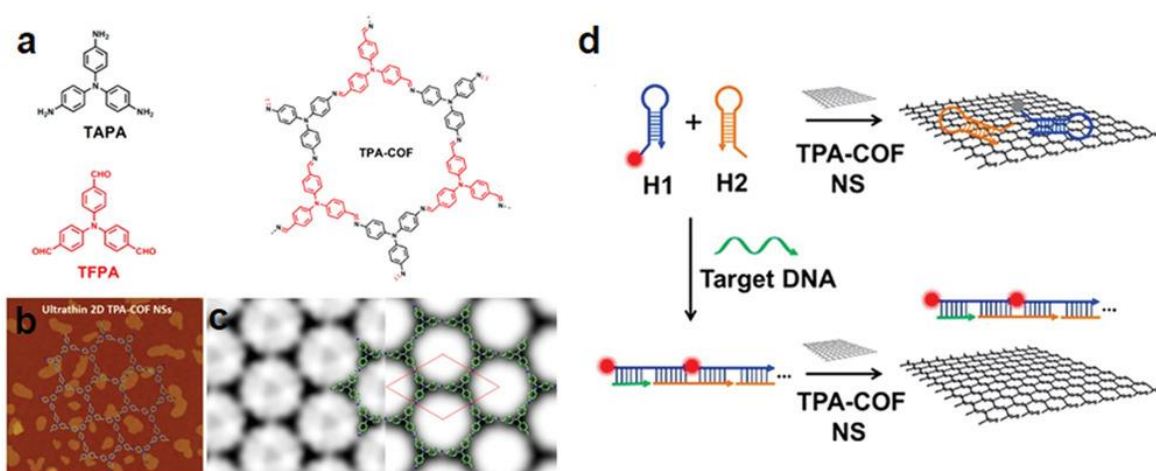


Figure 19. a.) Synthesis of extended hexagonal structure of TPA-COF; b.) AFM image of TPA-COF NS; c.) CTF-corrected HRTEM image of framework; d.) Illustration of TPA-COF NS-based fluorescence sensor for detection of DNA. Reprinted with permission from ref. 196.

(Copyright © 2017, American Chemical Society)

ENERGY STORAGE: COFs with high stacking density of π -orbitals arise opportunities in the field of carrier transport and mobilities in devices. The eclipsed stacked structure of COFs facilitates conduction via orbital interactions and also imparts excellent thermal stability without undergoing any phase transition, which is frequently observed in other conducting materials. Jiang research group reported first ever photoconductive eclipsed PPy-COF synthesized¹⁹⁸ by self-condensation of 2,7-pyrene diboronic acid. The long-range exciton delocalization was observed by sandwiched between Au and Al electrodes. The quick response along with large on off ratio as reflected by series of control experiments reflects the pivotal importance of stacked pyrene moieties in framework. To further improve the photoconductive performance, same research group incorporate first ever COF that integrate donor and acceptor in the building blocks as highlighted in benzothiadiazole acceptor and triphenylene donor. The enhance photoconductivity attributed to ambipolar electron and hole conduction with vertically ordered p-n heterojunctions¹⁹⁹.

Bein research group reported introduction of fullerene electron acceptor [6,6]-phenyl-C₆₁-butyric acid methyl ester (PCBM) into TT COF prepared by cocondensation of thieno[3,2-b]thiophene-2,5-diyl diboronic acid and polyol HHTP under solvothermal condition. The resultant hybrid composite formed by soaking framework in a PCBM chlorobenzene solution showed substantial photoresponse and effective charge transfer²⁰⁰. This infiltration strategy suffers from guest elusion from pore channel, to overcome this obstacle, Jiang and co-workers highlighted covalently bind guest molecule into framework by three component condensation reaction of 1,4-phenylenediboronic acid (BDDBA), 2,5-bis(azidomethyl)-1,4-phenylenediboronic acid (N₃-BDDBA) and (2,3,9,10,16,17,23,24-octahydroxyphthalocyaninato) zinc (ZnPc[OH]₈). The varying percentage of azide (X%N₃-ZnPc-COFs, X = 0, 10, 25, 50) moieties into framework with covalently anchoring C₆₀ translated into charge separation, photoenergy conversion and

photoinduced electron transfer¹¹⁶. Zhang research group reported ionic framework, ICOF-1 and ICOF-2 with sp^3 hybridized boron anionic centers and positively charged $(NMe_2)^+$ and Li^+ ions respectively (Figure 20). Both microporous frameworks exhibited surface area of $1022\text{ m}^2\text{g}^{-1}$ and $1259\text{ m}^2\text{g}^{-1}$ however, suffer from complex PXRD pattern led to absence of simulated crystal packing. Given the high porosity and Li^+ ions percentage, the frameworks showed conductivity of $3.05 \times 10^{-5}\text{ S cm}^{-1}$ at room temperature. Furthermore, the activation energy of same framework calculated to be 0.24 eV per atom, which is substantially higher than crystalline and polymer electrolyte⁴¹. Similar lithium infiltrated and counter ion-based frameworks reported by Feng research group²⁰¹ using γ -cyclodextrin and trimethylborate linked via tetrahedral tetrakis(spiroborate). The anionic framework with lithium counter ions exhibit conductivity up to 2.7 mS cm^{-1} at $30\text{ }^\circ\text{C}$. Polyelectrolyte based framework reported by Jiang and co-workers by infiltration of Li^+ ions using $LiClO_4$ into TPB-BMTP-COF prepared by condensation of 1,3,5-tris(4-aminophenyl) benzene (TPB) and 2,5-bis((2-methoxyethoxy) methoxy) terephthalaldehyde (BMTP) facilitates the association with alkali metal ions to induce ionic conduction and transportation with more than 3 orders of magnitude relative to other systems²⁰².

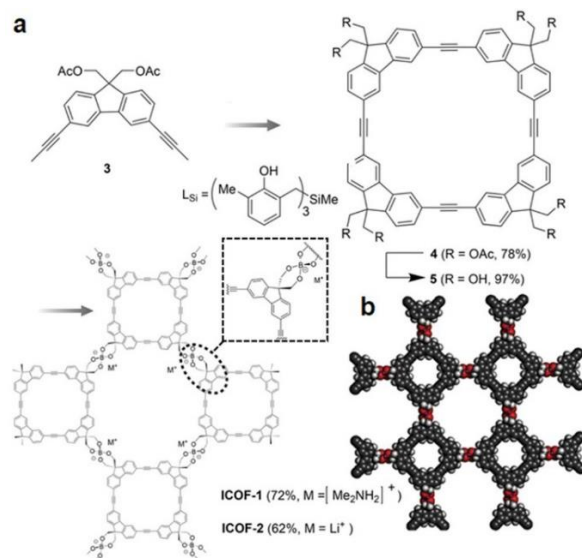


Figure 20. a.) Synthesis of ICOF-1 and ICOF-2; b.) Proposed structure of ICOF-2. Adapted with permission from ref. 41. (Copyright © 2016, Wiley-VCH Verlag GmbH & Co. KGaA, Weinheim)

The proton conduction in framework should be studied under the stable environment, which is primarily not only to protic and aprotic solvent but, also in high acidic and basic pH range. Banerjee research group synthesized²⁰³ azo functionalized stable framework by condensation of 4,4'-azodianiline (Azo) and triformylphloroglucinol (Tp) via β -ketoenamine-linkage. This strong linkage in the framework helps in maintaining structural stability and crystallinity at 9N HCl and 6N NaOH, a simple infiltration of H_3PO_4 in the stable Tp-Azo COF anchored on azo moieties and counter ions (H_2PO_4^-) stabilized via hydrogen bonds. This strong anchoring was further proven by the authors by highlighting the crystal structure of H_3PO_4 linked to azo center of 4-aminoazobenzene. With an uptake capacity of 5.4 wt%, PA@TpAzo COF showed proton conductivity of $6.7 \times 10^{-5} \text{ S cm}^{-1}$ under inert condition and $9.9 \times 10^{-4} \text{ S cm}^{-1}$ under 98% relative humidity. Polyoxometalates are well-known to exhibit proton conduction however, their solubility provides key problems to their real-world applications. COFs as a decorating platform will provide assistance to overcome this barrier, for instance, Zhu research group synthesized ionic EB-COF:Br by condensation reaction of 1,3,5-triformylphloroglucinol and ethidium bromide (EB). The cationic monomer in COF imparts essential characteristics led to ion exchange with $\text{H}_3\text{PW}_{12}\text{O}_{40}$ substantially improved proton conduction with $3.32 \times 10^{-3} \text{ S cm}^{-1}$ at 97% relative humidity. In comparison to the hybrid system, $\text{H}_3\text{PW}_{12}\text{O}_{40}$ and EB-COF:Br mixture exhibited smaller proton conduction ($3.2 \times 10^{-5} \text{ S cm}^{-1}$), which is profoundly due to the uniform distribution of bromide anions²⁰⁴ (Figure 21). In addition to this, Dichtel research group reported immobilization of 2,6-diaminoanthraquinone, a redox active species in hydrostable 2D β -ketoenamines linked COF²⁰⁵.

Same research also highlighted integration of conductive polymer, poly(3,4-ethylenedioxythiophene) (PEDOT) within the 1D pore channel of framework by electropolymerizing of 3,4-ethylenedioxythiophene (EDOT). The hybrid framework with $1\mu\text{m}$ thickness exhibited considerably improved electrochemical performance. Most importantly, the hybrid material showed stable capacitance up to 10,000 cycles²⁰⁶. To further improved the electrical conductivity, Jiang and co-workers imitate graphene conductive material by synthesizing sp^2 carbon-conjugated COF (C=C bond) under the principle of reticular chemistry⁵⁶. The π -conjugated crystalline material synthesized using tetrakis(4-formylphenyl) pyrene and 1,4-phenylenediacetonitrile exhibited semiconductor with a band gap of 1.9 eV, which increases on chemical oxidation of I_2 .

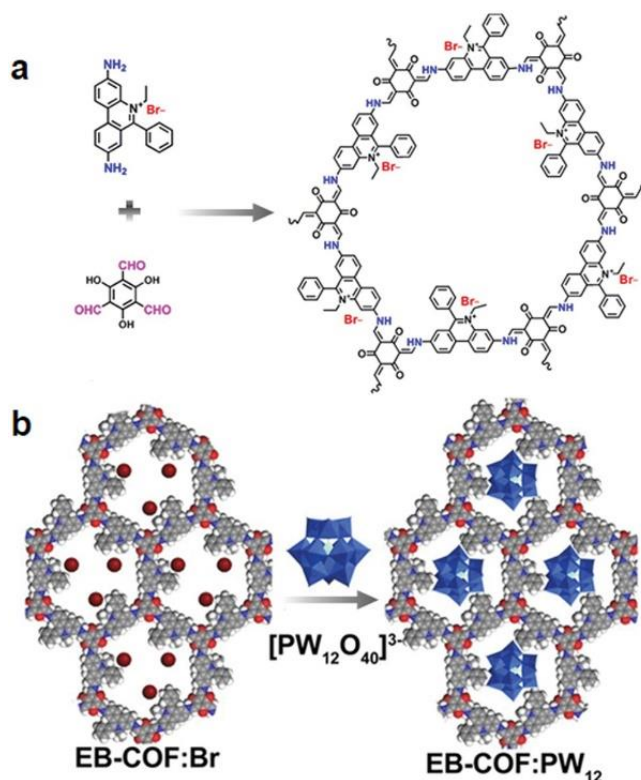


Figure 21. a.) Schematic representation of EB-COF:Br synthesis; b.) $[\text{PW}_{12}\text{O}_{40}]^{3-}$ doping in ionic framework. Reproduced with permission from ref. 204. (Copyright © 2016, American Chemical Society)

COFs thin films are usually accessed by three prominent strategies. Firstly, solvothermal synthesis, COFs directly grown in solid support, however, this method produces crystalline films with pores oriented perpendicular to the substrate, but, suffer from various disadvantage such as difficult to remove from the support and scale up. Secondly, interfacial polymerization, in this technique monomer or catalysts are dissolved separately in two immiscible solvents such that COF formation occur at the interface with controllable thickness, however, poor crystallinity is often obtained with thickness more than 50 nm. Thirdly, exfoliation and reconstitution of COF powder, this strategy provide direct route to the film morphology with precisely tuned dimensions. Dichtel research group highlighted first oriented thin COF films on substrate-supported single layer graphene (SLG), thereby provide suitable substrate for the COF growth via favourable π -interactions²⁰⁷. Shortly thereafter, same group reported large pore size frameworks based on large chromophore were prepared as oriented thin films on substrate-supported SLG²⁰⁸. Bein and co-workers incorporate mesoporous framework (BDT-COF) prepared by condensation of benzodithiophene-containing diboronic acid (BDTBA) and 2,3,6,7,10,11-hexahydroxytriphenylene (HHTP) with various polycrystalline surfaces characterized by PXRD, SEM, TEM, 2D grazing incidence diffraction (GID)²⁰⁹. The electron-donor / acceptor host-guest systems obtained by infiltration of BDT-COF films with soluble fullerene derivatives such as [6,6]-phenyl C_{61} butyric acid methyl ester (PCBM) susceptible electron transfer by photoluminescence quenching due to charge transfer between host and guest.

Wang and co-workers reported novel ways of synthesizing 2D COF thin films at the oil / water / hydrogel interfaces with controllable thickness from 4 to 150 nm and young's modulus (25.9 ± 0.6 GPa) by AFM. Furthermore, COF film-based hybrid material used as selective photoelectrochemical sensor for Ru^{3+} ions²¹⁰. Wang and co-workers reported 2D NT-COF by integration of electron-rich triphenyl amine (TPA) and electron-poor naphthalenediimide (NDI) in crystalline "bnn" topology, $1.22 \text{ cm}^3\text{g}^{-1}$ pore volume and $1276 \text{ m}^2\text{g}^{-1}$ surface area. The successful synthesis was further verified by FT-IR, NMR, SEM and TEM. Due to the nature of monomers, the synergistic effect in framework between intramolecular charge transfer, from the TPA to the NDI and reversible electrochemical performance provide essential basis to direct solar-to-electrochemical energy conversion / storage. The sheet-like layered structure of NT-COF serve as cathode materials in a solar Li^+ ion a battery under light irradiation exhibited increased discharge voltage from 2.42 V to 2.96 V (0.5 V increase), decreased charge voltage by 0.5 V, from 3.04 V to 2.53 V and more importantly 38.7 % extra battery efficiency, from 78.3 % to 117 %²¹¹.

Wang and co-workers reported synthesis of sp^2 carbon-conjugated COF by condensation of 5,10,15,20-tetrakis(4-benzaldehyde) porphyrin (p-Por-CHO) and 1,4-phenylenediacetonitrile (PDAN) via Knoevenagel condensation reaction. The AA stacked structure was confirmed by PXRD pattern, structurally investigated by FT-IR, NMR with thermal stability up to 250 °C and also under harsh condition such as 9 M HCl, 9 M NaOH. The framework exhibited porosity with BET surface area of $689 \text{ m}^2\text{g}^{-1}$ and pore size of 1.8 nm. The metal-free olefin-linked heterogeneous catalyst serves as photocatalyst for the visible-light-induced aerobic oxidation of amines to imines²¹². Zhao research group reported highly conjugated imine-linked three-dimensional SP-3D-COF 1 and SP-3D-COF 2 frameworks by condensation of 3,3',6,6'-tetraamine-9,9'-spirobifluorene with terephthalaldehyde and 4,4'-biphenyldicarbaldehyde in o-DCB / n-BuOH /

AcOH respectively. SP-3D-COFs exhibited P_{42}/NNM space group with “dia” topology with degree of interpenetration higher than 6 or 7 and structurally verified using physiochemical analysis. The authors investigated advanced photoelectric properties for solar energy harvesting by doping frameworks into $CH_3NH_3PbI_3$ perovskite layer with an average 18.34 % power conversion efficiency (PCE) and maximum PCE of 19.07 % for SP-3D-COF 1. However, an average PCE of 18.68 % for SP-3D-COF 2, more importantly, the average PCE over reference undoped PSC was highly improved by 15.9 % and 18.0 % for SP-3D-COF 1 and SP-3D-COF 2 doping²¹³. Moreover, the mechanistic studies of perovskite-SP-3D-COF interactions was studied from both experimental and computational studies which in turn, helps in understanding the photoresponsive perovskite behaviour.

CONCLUSION: Covalent organic frameworks constructed by the dynamic covalent linkage of building block units using range of functionalities under the principle of reticular chemistry. The extensive work carried out during number of years in the field of porous materials especially COFs substantially develop the field from various viewpoints drawing an attention of different communities in chemistry or interdisciplinary fields. Fundamentally, peculiar properties attached with dynamic covalent chemistry bestow in designing frameworks under the shade of robust covalent bonds led to thermal stability which is one of the important properties by far to address future challenges and industrialization. The geometric features associated with building blocks entirely decide the topology, morphology, pore nature of frameworks, most of the times, introduction of specific properties in building block either tedious or impossible but, can be accessed through pore surface engineering. Pore surface engineering either in context of metal complexation or chemical conversion in regular pore channel comes from well-established

coordination chemistry or organic chemistry. This metal complexation plays pivotal role in the field of heterogeneous catalysis, which not only overcomes the disadvantages attach to homogeneous catalysis such as residual waste, recyclability or reusability but, also address some of the key organic conversion and name reactions including Suzuki-Miyaura coupling, Prins reaction, C-H borylation, Henry reaction, CO₂ reduction, CO₂ insertion and many more as discussed in this review. Furthermore, pore surface engineering of functional groups plays critical role in environmental remediation, selective uranium extraction via introduction of amidoxime functionalities or thiol functionalities to capture mercury ions in record uptake values (0.1 ppb), far less than acceptable limit for drinking water (2 ppb) with excellent recyclability. This illustrates the impact of pore surface engineering which originates from signature properties of COFs especially high porosity, thermal and chemical stability. The flexibility and potential of this approach has been extensively summarized in the functional group interconversion to bring structural diversity, which in turn, open the role of framework in rapidly growing challenges.

The vast library of organic precursor units bearing different binding units is in itself illuminated in the structural and functional diversity of COFs. This highlighted in gas adsorption and separation as demonstrated in 3D COF-102 and COF-103 with an exceptional hydrogen uptake of 72.4 mg g⁻¹ and 70.5 mg g⁻¹ respectively. Moreover, the impact of spillover effect, Lewis acid-base adducts (B—N) and incorporation of ionic precursor units substantially affect the selective gas adsorption such as CO₂ over CH₄. COFs porosity is also responsible for high uptake of commercially available drug. The favorable interactions between host and guest helps in release of various drug molecules (ibuprofen, captopril, caffeine and 5-fluorouracil) over days instead of one-time shot. Furthermore, enzyme encapsulation in framework induces stability of enzymes inhibiting denaturation exhibiting catalytic reactions with excellent reusability without any

hindrance in morphology or crystallinity. These essential characteristics along with high density of hydrogen bonding synthons in COFs makes the porous materials as an excellent selective sensor for nitro compounds over other compounds. The presence of chelating functionalities exhibited strong and selective quenching of Cu^{2+} and Hg^{2+} over other transition metal ions. The role of electrostatic, π - π stacking interactions stich to frameworks helps in distinguishing dsDNA from ssDNA and makes framework as good energy storage. Within this respect, the development of fabricating COFs architectures and control structure still remain a scientific challenge along with scalable synthesis, controlled morphology, biocompatibility, hydrolytic stability is still a challenging task in front of research communities. In addition to this, few other challenges are mentioned below:

1. Building block exchange and sequential pore surface engineering of COFs to further embellish the backbone by innumerable functionalities play central role to address growing number of applications. This phase of COFs is still in its infancy; therefore, in-depth study is of profound importance.
2. The library of metal-linked organic scaffolds to construct catalytically active COFs via *de novo* strategy using dynamic covalent linkage is very sporadic. Therefore, enriching the library of monomer units is of vital importance to widened the scope of COFs for catalytic applications.
3. 2D COFs have been successfully synthesized by using dynamic covalent chemistry, however, translating this enrich chemistry into 3D COFs is still in its early stage. One of the core challenges is crystallization problem which emanates from imbalance between strong covalent bond and reversible linkages.

4. Detailed mechanistic study to form 3D COFs at room temperature is still unexplored. The organic scaffold to constructs 3D frameworks is limited, thereby, restricted the number of topologies exist in this field.

CONFLICTS OF INTEREST: The author declares no conflicts of interest.

ACKNOWLEDGEMENTS: The authors acknowledge the University of South Florida and NSF (CBET-1706025) for financial support. We also extend our appreciation to the Distinguished Scientist Fellowship Program (DSFP) at King Saud University for funding this work partially.

REFERENCES

1. P. J. Waller, F. Gándara and O. M. Yaghi, *Acc. Chem. Res.* 2015, **48**, 3053-3063.
2. J. M. Lehn, *Chem.-Eur. J.* 1999, **5**, 2455-2463.
3. H. Li, M. Eddaoudi, T. L. Groy and O. M. Yaghi, *J. Am. Chem. Soc.* 1998, **120**, 8571-8572.
4. S. S. Chui, S. M. Lo, J. P. Charmant, A. G. Orpen and I. D. Williams, *Science* 1999, **283**, 1148-1150.
5. H. Li, M. Eddaoudi, M. O'Keeffe and O. M. Yaghi, *Nature* 1999, **402**, 276-279.
6. A. P. Côte, I. A. Benin, N. W. Ockwig, M. O'Keeffe and O. M. Yaghi, *Science* 2005, **310**, 1166-1170.
7. S. Das, P. Heasman, T. Ben and S. Qui, *Chem. Rev.* 2017, **117**, 1515-1563.
8. A. G. Slater and A. I. Cooper, *Science* 2015, **348**, 988-998.
9. U. Diaz and A. Corma, *Coord. Chem. Rev.* 2016, **311**, 85-124.

10. K. E. Maly, *J. Mater. Chem.* 2009, **19**, 1781-1787.
11. A. Thomas, *Angew. Chem. Int. Ed.* 2010, **49**, 8328-8344.
12. X. Feng, X. Ding and D. Jiang, *Chem. Soc. Rev.* 2012, **41**, 6010-6022.
13. R. P. Bisbey and W. R. Dichtel, *ACS Cent. Sci.* 2017, **3**, 533-543.
14. F. Beuerle and B. Gole, *Angew. Chem. Int. Ed.* 2018, **57**, 4850-4878.
15. Y. Jin, Y. Hu and W. Zhang, *Nat. Rev. Chem.* 2017, **1**, 0056.
16. C. S. Diercks and O. M. Yaghi, *Science* 2017, **355**, No. eaal1585.
17. P. J. Waller, F. Gandara and O. M. Yaghi, *Acc. Chem. Res.* 2015, **48**, 3053-3063.
18. S.-Y. Ding and W. Wang, *Chem. Soc. Rev.* 2013, **42**, 548-568.
19. T. Ma, E. A. Kapustin, S. X. Yin, L. Liang, Z. Zhou, J. Niu, H. Li, Y. Wang, J. Su, J. Li, X. Wang, W. D. Wang, W. Wang, J. Sun and O. M. Yaghi, *Science* 2018, **361**, 48-52.
20. L. Pauling, *The Nature of the Chemical Bond*, 2nd ed.; Cornell University Press: New York, 1940; 7-10.
21. R. B. Woodward, *Pure Appl. Chem.* 1973, **33**, 145-178.
22. A. Eschenmoser and C. E. Wintner, *Science* 1977, **196**, 1410-1420.
23. S. J. Rowan, S. J. Cantrill, G. R. L. Cousins, J. K. M. Sanders and J. F. Stoddart, *Angew. Chem. Int. Ed.* 2002, **41**, 898-952.
24. Y. Jin, Q. Wang, P. Taynton and W. Zhang, *Acc. Chem. Res.* 2014, **47**, 1575-1586.
25. O. M. Yaghi, *Mater. Front. J.* 2019, **3**, 1-18.
26. O. M. Yaghi, *ACS Cent. Sci.* DOI: 10.1021/acscentsci.9b00750.
27. Y. Liu, M. O'Keeffe, M. M. J. Treacy and O. M. Yaghi, *Chem. Soc. Rev.* 2018, **47**, 4642-4664.

28. B. Rungtaweeworanit, C. S. Diercks, M. J. Kalmutzki and O. M. Yaghi, *Faraday Discuss.* 2017, **201**, 9-45.
29. K. E. Cordova and O. M. Yaghi, *Mater. Chem. Front.* 2017, **1**, 1304-1309.
30. N. Huang, P. Wang and D. Jiang, *Nat. Rev. Mater.* 2016, **1**, 16068.
31. J. Jiang, Y. Zhao and O. M. Yaghi, *J. Am. Chem. Soc.* 2016, **138**, 3255-3265.
32. S. Kandambeth, K. Dey and R. Banerjee, *J. Am. Chem. Soc.* 2019, **141**, 1807-1822.
33. C. S. Diercks, M. J. Kalmutzki and O. M. Yaghi, *Molecules* 2017, **22**, 1575-1580.
34. S. J. Lyle, P. J. Waller and O. M. Yaghi, *Trends Chem.* 2019, **1**, 172-184.
35. F. Zhao, H. Liu, S. D. R. Mathe, A. Dong and J. Zhang, *Nanomaterials* 2018, **8**, 15-64.
36. Y. Song, Q. Sun, B. Aguila and S. Ma, *Adv. Sci.*, 2019, **6**, 1801410.
37. M. S. Lohse and T. Bein, *Adv. Funct. Mater.* 2018, **28**, 1705553.
38. H. M. El-Kaderi, J. R. Hunt, J. L. Mendoza-Cortés, A. P. Côté, R. E. Taylor, M. O'Keeffe and O. M. Yaghi, *Science* 2007, **316**, 268-272.
39. E. L. Spitler, B. T. Koo, J. L. Novotney, J. W. Colson, F. J. Uribe-Romo, G. D. Gutierrez, P. Clancy and W. Dichtel, *J. Am. Chem. Soc.* 2011, **133**, 19416-19421.
40. J. R. Hunt, C. J. Doonan, J. D. Levanjie, A. P. Côté and O. M. Yaghi, *J. Am. Chem. Soc.* 2008, **130**, 11872-11873.
41. Y. Du, H. Yang, J. M. Whiteley, S. Wan, Y. Jin, S. H. Lee and W. Zhang, *Angew. Chem. Int. Ed.* 2016, **55**, 1737-1741.
42. F. J. Uribe-Romo, J. R. Hunt, H. Furukawa, C. Klock, M. O'Keeffe and O. M. Yaghi, *J. Am. Chem. Soc.* 2009, **131**, 4570-4571.
43. S. Kandameth, A. Mallick, B. Lukose, M. V. Mane, T. Heine and R. Banerjee, *J. Am. Chem. Soc.* 2012, **134**, 19524-19527.

44. S. Chandra, S. Kandambeth, B. P. Biswal, B. Lukose, S. M. Kunjir, M. Chaudhary, R. Babarao, T. Heine and R. Banerjee, *J. Am. Chem. Soc.* 2013, **135**, 17853-17861.
45. B. P. Biswal, S. Chandra, S. Kandambeth, B. Lukose, T. Hein and R. Banerjee, *J. Am. Chem. Soc.* 2013, **135**, 5328-5331.
46. S. Karak, S. Kandambeth, B. P. Biswal, H. S. Sasmal, S. Kumar, P. Pachfule and R. Banerjee, *J. Am. Chem. Soc.* 2017, **139**, 1856-1862.
47. S. Dalapati, S. Jin, J. Gao, Y. Xu, A. Nagai and D. Jiang, *J. Am. Chem. Soc.* 2013, **135**, 17310-17313.
48. J. Guo, Y. Xu, S. Jin, L. Chen, T. Kaji, Y. Honsho, M. A. Addicoat, J. Kim, A. Saeki, H. Ihee, S. Seki, S. Irle, M. Hiramoto, J. Gao and D. Jiang, *Nat. Commun.* 2013, **4**, 2736.
49. A. Nagai, X. Chen, X. Feng, X. Ding, Z. Guo and D. Jiang, *Angew. Chem. Int. Ed.* 2013, **52**, 3770-3774.
50. L. Grill, M. Dyer, L. Lafferentz, M. Persson, M. V. Peters and S. Hecht, *Nat. Nanotechnol.* 2007, **2**, 687-691.
51. M. O. Blunt, J. C. Russell, N. R. Champness and P. H. Beton, *Chem. Commun.* 2010, **46**, 7157-7159.
52. C. R. Larrea and C. J. Baddeley, *ChemPhysChem* 2016, **17**, 971-975.
53. T. Faury, S. Clair, M. Abel, F. Dumur, D. Gigmes and L. Porte, *J. Phys. Chem. C* 2012, **116**, 4819-4823.
54. K. J. Shi, D. W. Yuan, C. X. Wang, C. H. Shu, D. Y. Li, Z. L. Shi, X. Y. Wu and P. N. Liu, *Org. Lett.* 2016, **18**, 1282-1285.

55. A. C. Marele, R. Mas-Balleste, L. Terracciano, J. Rodriguez-Fernandez, I. Berlanga, S. S. Alexandre, R. Otero, J. M. Gallego, F. Zamora and J. M. Gomez-Rodriguez, *Chem. Commun.* 2012, **48**, 6779-6781.
56. E. Jin, M. Asada, Q. Xu, S. Dalapati, M. A. Addicoat, M. A. Brady, H. Xu, T. Nakamura, T. Heine, Q. Chen and D. Jiang, *Science* 2017, **357**, 673-676.
57. H. Lyu, C. S. Diercks, C. Zhu and O. M. Yaghi, *J. Am. Chem. Soc.* 2019, **141**, 6848-6852.
58. K. T. Jackson, T. E. Reich and H. M. El-Kaderi, *Chem. Commun.* 2012, **48**, 8823-8825.
59. D. Beaudoin, T. Maris and J. S. Wuest, *Nat. Chem.* 2013, **5**, 830-834.
60. X. Chen, M. Addicoat, E. Jin, H. Xu, T. Hayashi, F. Xu, N. Huang, S. Irle and D. Jiang, *Sci. Rep.* 2015, **5**, 14650.
61. Y. Zeng, R. Zou, Z. Luo, H. Zhang, X. Yao, X. Ma, R. Zou and Y. Zhao, *J. Am. Chem. Soc.* 2015, **137**, 1020-1023.
62. P. Kuhn, M. Antonietti and A. Thomas, *Angew. Chem. Int. Ed.* 2008, **47**, 3450-3453.
63. N. L. Campbell, R. Clowes, L. K. Ritchie and A. I. Cooper, *Chem. Mater.* 2009, **21**, 204-206.
64. M. Dogru, A. Sonnauer, A. Gavryushin, P. Knochel and T. Bein, *Chem. Commun.* 2011, **47**, 1707-1709.
65. J. W. Colson, A. R. Woll, A. Mukherjee, M. P. Levendorf, E. L. Spitler, V. P. Shields, M. G. Spencer, J. Park and W. R. Dichtel, *Science* 2011, **332**, 228-231.
66. E. L. Spitler, J. W. Colson, F. J. Uribe-Romo, A. R. Woll, M. R. Giovino, A. Saldivar and W. R. Dichtel, *Angew. Chem. Int. Ed.* 2012, **51**, 2623-2627.
67. S. Y. Ding, X. H. Cui, J. Feng, G. Lu and W. Wang, *Chem. Commun.* 2017, **53**, 11956-11959.

68. M. Matsumoto, R. R. Dasari, W. Ji, C. H. Feriante, T. C. Parker, S. R. Marder and W. R. Dichtel, *J. Am. Chem. Soc.* 2017, **139**, 4999-5002.
69. A. Werner, *Z. Anorg. Allg. Chem.* 1893, **3**, 267-330.
70. Y. Kinoshita, I. Matsubara and Y. Saito, *Bull. Chem. Soc. Jpn*, 1959, **32**, 1216-1221.
71. Y. Kinoshita, I. Matsubara, T. Higuchi and Y. Saito, *Bull. Chem. Soc. Jpn*, 1959, **32**, 1221-1226.
72. N. Huang, L. Zhai, D. E. Coupry, M. A. Addicoat, K. Okushita, K. Nishimura, T. Heine and D. Jiang, *Nat. Commun.* 2016, **7**, 12325.
73. A. P. Côté, H. M. El-Kaderi, H. Furukawa, J. R. Hunt and O. M. Yaghi, *J. Am. Chem. Soc.* 2007, **129**, 12914-12915.
74. S.-B. Yu, H. Lyu, J. Tian, H. Wang, D.-W. Zhang, Y. Liu and Z.-T. Li, *Polym. Chem.* 2016, **7**, 3392-3397.
75. S. Jin, K. Furukawa, M. Addicoat, L. Chen, S. Takahashi, S. Irle, T. Nakamura and D. Jiang, *Chem. Sci.* 2013, **4**, 4505-4511.
76. R. W. Tilford, S. J. Mugavero, P. J. Pellechia and J. J. Lavigne, *Adv. Mater.* 2008, **20**, 2741-2746.
77. A. Nagai, Z. Guo, X. Feng, S. Jin, X. Chen, X. Ding and D. Jiang, *Nat. Commun.* 2011, **2**, 536.
78. Z.-F. Pang, S.-Q. Xu, T.-Y. Zhou, R.-R. Liang, T.-G. Zhan and X. Zhao, *J. Am. Chem. Soc.* 2016, **138**, 4710-4713.
79. L. Ascherl, T. Sick, J. T. Margraf, S. H. Lapidus, M. Calik, C. Hettstedt, K. Karaghisoff, M. Dblinger, T. Clark, K. W. Chapman, F. Auras and T. Bein, *Nat. Chem.* 2016, **8**, 310-316.

80. Y. Zhu, S. Wan, Y. Jin and W. Zhang, *J. Am. Chem. Soc.* 2015, **137**, 13772-13775.
81. S. Dalapati, E. Jin, M. Addicoat, T. Heine and D. Jiang, *J. Am. Chem. Soc.* 2016, **138**, 5797-5800.
82. L. A. Baldwin, J. W. Crowe, M. D. Shannon, C. P. Jaroniec and P. L. McGrier, *Chem. Mater.* 2015, **27**, 6169-6172.
83. Y. P. Mo, X. H. Liu and D. Wang, *ACS Nano* 2017, **11**, 11694-11700.
84. B. T. Koo, W. R. Dichtel and P. A. Clancy, *J. Mater. Chem.* 2012, **22**, 17460-17469.
85. J. W. Buchler, In porphyrins, ed. D. Dolphin, Academic Press, New York, 1978, ch. 10, vol. 1, p. 389.
86. K. M. Kadish, K. M. Smith and R. Guilard, *The Porphyrin Handbook*, Academic Press, San Diego, CA, 2000, vol. 3.
87. W. Seo, D. L. White and A. Star, *Chem.-Eur. J.* 2017, **23**, 5652-5657.
88. E. M. Johnson, R. Haiges and S. C. Marinescu, *ACS Appl. Mater. Interfaces* 2018, **10**, 37919-37927.
89. K. Srinivasu and S. K. Ghosh, *J. Phys. Chem. C* 2013, **117**, 26021-26028.
90. L. A. Baldwin, J. W. Crowe, D. A. Pyles and P. L. McGrier, *J. Am. Chem. Soc.* 2016, **138**, 15134-15137.
91. S.-Y. Ding, J. Gao, Q. Wang, Y. Zhang, W.-G. Song, C.-Y. Su and W. Wang, *J. Am. Chem. Soc.* 2011, **133**, 19816-19822.
92. L. Chen, L. Zhang, Z. Chen, H. Liu, R. Luque and Y. Li, *Chem. Sci.* 2016, **7**, 6015-6020.
93. D. Sun, S. Jang, S.-J. Yim, L. Ye and D.-P. Kim, *Adv. Funct. Mater.* 2018, **28**, 1707110.
94. Y. Hou, X. Zhang, J. Sun, S. Lin, D. Qi, R. Hong, D. Li, X. Xiao and J. Jiang, *Microporous Mesoporous Mater.* 2015, **214**, 108-114.

95. W. Leng, Y. Peng, J. Zhang, H. Lu, X. Feng, R. Ge, B. Dong, B. Wang, X. Hu and Y. Gao, *Chem.-Eur. J.* 2016, **22**, 9087-9091.
96. W. Leng, R. Ge, B. Dong, C. Wang and Y. Gao, *RSC Adv.* 2016, **6**, 37403-37406.
97. S. Lin, Y. Hou, X. Deng, H. Wang, S. Sun and X. Zhang, *RSC Adv.* 2015, **5**, 41017-41024.
98. P. Pachfule, M. K. Panda, S. Kandambeth, S. M. Shivaprasad, D. D. Díaz and R. Banerjee, *J. Mater. Chem. A.* 2014, **2**, 7944-7956
99. A. de la Peña Ruigómez, D. Rodríguez-San-Miguel, K. C. Stylianou, M. Cavallini, D. Gentili, F. Liscio, S. Milita, O. M. Roscioni, M. L. Ruiz-González, C. Carbonell, D. Maspoch, R. Mas-Ballesté, J. L. Segura and F. Zamora, *Chem.-Eur. J.* 2015, **21**, 10666-10670.
100. J. Romero, D. Rodriguez-San-Miguel, A. Ribera, R. Mas-Ballesté, T. F. Otero, I. Manet, F. Licio, G. Abellán, F. Zamora and E. Coronado, *J. Mater. Chem. A.* 2017, **5**, 4343-4351.
101. H. B. Aiyappa, J. Thote, D. B. Shinde, R. Banerjee and S. Kurungot, *Chem. Mater.* 2016, **28**, 4375-4379.
102. Q. Sun, B. Aguila, J. Perman, N. Nguyen and S. Ma, *J. Am. Chem. Soc.* 2016, **138**, 15790-15796.
103. M. Mu, Y. Wang, Y. Qin, X. Yan, Y. Li and L. Chen, *ACS Appl. Mater. Interfaces* 2017, **9**, 22856-22863.
104. P. G. Cozzi, *Chem. Soc. Rev.* 2004, **33**, 410-421.
105. T. P. Yoon, E. N. Jacobsen, *Science* 2003, **299**, 1691-1693.
106. L.-H. Li, X.-L. Feng, X.-H. Cui, Y.-X. Ma, S.-Y. Ding and W. Wang, *J. Am. Chem. Soc.* 2017, **139**, 6042-6045.

107. H. Vardhan, G. Verma, S. Ramani, A. Nafady, A. M. Al-Enizi, Y. Pan, Z. Yang, H. Yang and S. Ma, *ACS Appl. Mater. Interfaces*, 2019, **11**, 3070-3079.
108. H. Vardhan, L. Hou, E. Yee, A. Nafady, A. M. Al-Enizi, Y. Pan, Z. Yang and S. Ma, *ACS Sustainable Chem. Eng.* 2019, **7**, 4878-4888.
109. Y. Liu, Y. Ma, Y. Zhao, X. Sun, F. Gándara, H. Furukawa, Z. Liu, H. Zhu, C. Zhu, K. Suenaga, P. Oleynikov, A. S. Alshammari, X. Zhang, O. Terasaki and O. M. Yaghi, *Science* 2016, **351**, 365-369.
110. H. Wang, F. Jiao, F. Gao, Y. Lv, Q. Wu, Y. Zhao, Y. Shen, Y. Zhang and X. Qian, *Talanta* 2017, **166**, 133-140.
111. Q. Sun, B. Aguila and S. Ma, *Mater. Chem. Front.* 2017, **1**, 1310-1316.
112. Y. Yang, M. Faheem, L. Wang, Q. Meng, H. Sha, N. Yang, Y. Yuan and G. Zhu, *ACS Cent. Sci.* 2018, **4**, 748-754.
113. F. J. Uribe-Romo, C. J. Doonan, H. Furukawa, K. Oisaki and O. M. Yaghi, *J. Am. Chem. Soc.* 2011, **133**, 11478-11481.
114. W. Zhang, P. Jiang, Y. Wang, J. Zhang, Y. Gao and P. Zhang, *RSC Adv.* 2014, **4**, 51544-51547.
115. T. Kundu, J. Wang, Y. Cheng, Y. Du, Y. Qian, G. Liu and D. Zhao, *Dalton Trans.* 2018, **47**, 13824-13829.
116. L. Chen, K. Furukawa, J. Gao, A. Nagai, T. Nakamura, Y. Dong and D. Jiang, *J. Am. Chem. Soc.* 2014, **136**, 9806-9809.
117. N. Huang, R. Krishna and D. Jiang, *J. Am. Chem. Soc.* 2015, **137**, 7079-7082.
118. F. Xu, H. Xu, X. Chen, D. Wu, Y. Wu, H. Liu, C. Gu, R. Fu and D. Jiang, *Angew. Chem. Int. Ed.* 2015, **54**, 6814-6818.

119. H. Xu, J. Gao and D. Jiang, *Nat. Chem.* 2015, **7**, 905-912.
120. S. Royuela, E. García-Garrido, M. Martín arroyo, M. J. Mancheño, M. M. Ramos, D. González-Rodríguez, A. Samoza, F. Zamora and J. L. Segura, *Chem. Commun.* 2018, **54**, 8729-8732.
121. L. Merí-Bofí, S. Royuela, F. Zamora, M. L. Ruiz-González, J. L. Segura, R. Muñoz-Olivas and M. J. Mancheño, *J. Mater. Chem. A.* 2017, **5**, 17973-17981.
122. D. N. Bunck and W. R. Dichtel, *Chem. Commun.* 2013, **49**, 2457-2459.
123. Q. Sun, B. Aguila, J. Perman, L. D. Earl, C. W. Abney, Y. Cheng, H. Wei, N. Nguyen, L. Wojtas and S. Ma, *J. Am. Chem. Soc.* 2017, **139**, 2786-2793.
124. Q. Sun, B. Aguila, J. A. Perman, T. Butts, F.-S. Xiao and S. Ma, *Chem.* 2018, **4**, 1726-1739.
125. Q. Sun, B. Aguila, L. D. Earl, C. W. Abney, L. Wojtas, P. K. Thallapally and S. Ma, *Adv. Mater.* 2018, **30**, 1705479.
126. B. Zhang, M. Wei, H. Mao, X. Pei, S. A. Alshimri, J. A. Reimer and O. M. Yaghi, *J. Am. Chem. Soc.* 2018, **140**, 12715-12719.
127. X. Guan, H. Li, Y. Ma, M. Xue, Q. Fang, Y. Yan, V. Valtchev and S. Qiu, *Nat. Chem.* 2019, **11**, 587-594.
128. W. Ji, L. Xiao, Y. Ling, C. Ching, M. Matsumoto, R. P. Bisbey, D. E. Helbling and W. R. Dichtel, *J. Am. Chem. Soc.* 2018, **140**, 12677-12681.
129. H.-S. Xu, S.-Y Ding, W.-K. An, H. Wu and W. Wang, *J. Am. Chem. Soc.* 2016, **138**, 11489-11492.
130. N. Huang, X. Chen, R. Krishna and D. Jiang, *Angew. Chem. Int. Ed.* 2015, **54**, 2986-2990.

131. S. Zhao, B. Dong, R. Ge, C. Wang, X. Song, W. Ma, Y. Wang, C. Hao, X. Guo and Y. Gao, *RSC Adv.* 2016, **6**, 38774-38781.
132. B. Dong, L. Wang, S. Zhao, R. Ge, X. Song, Y. Wang and Y. Gao, *Chem. Commun.* 2016, **52**, 7082-7085.
133. Z.-J. Mu, X. Ding, Z.-Y. Chen and B.-H Han, *ACS Appl. Mater. Interfaces* 2018, **10**, 41350-41358.
134. Q. Lu, Y. Ma, H. Li, X. Guan, Y. Yusran, M. Xue, Q. Fang, Y. Yan, S. Qiu and V. Valtchev, *Angew. Chem. Int. Ed.* 2018, **57**, 6042-6048.
135. S. Rager, M. Dogru, V. Werner, A. Gavryushin, M. Götz, H. Engelke, D. D. Medina, P. Knochel and T. Bein, *CrystEngComm.* 2017, **19**, 4886-4891.
136. M. S. Lohse, T. Stassin, G. Naudin, S. Wuttke, R. Ameloot, D. De Vos, D. D. Medina and T. Bein, *Chem. Mater.* 2016, **28**, 626-631.
137. D. B. Shinde, H. B. Aiyappa, M. Bhadra, B. P. Biswal, P. Wadge, S. Kandambeth, B. Garai, T. Kundu, S. Kurungot and R. Banerjee, *J. Mater. Chem. A*, 2016, **4**, 2682-2690.
138. W. Zhong, R. Sa, L. Li, Y. He, L. Li, J. Bi, Z. Zhuang, Y. Yu and Z. Zou, *J. Am. Chem. Soc.* 2019, **141**, 7615-7621.
139. Z. Zou, W. Zhong, K. Cui, Z. Zhuang, L. Li, L. Li, J. Bi and Y. Yu, *Chem. Commun.*, 2018, **54**, 9977-9980.
140. H. Vardhan, Y. Pan, Z. Yang, G. Verma, A. Nafady, A. M. Al-Enizi, T. M. Alotaibi, O. A. Almaghrabi and S. Ma, *APL Materials* 2019, **7**, 101111.
141. J. L. Segura, S. Royuela and M. M. Ramos, *Chem. Soc. Rev.* 2019, **48**, 3903-3945.
142. P. J. Waller, S. J. Lyle, T. M. Osborn Popp, C. S. Diercks, J. Am. Reimer and O. M. Yaghi, *J. Am. Chem. Soc.* 2016, **138**, 15519-15522.

143. X. Han, J. Huang, C. Yuan, Y. Liu and Y. Cui, *J. Am. Chem. Soc.* 2018, **140**, 892-895.
144. S. Wang, Q. Wang, P. Shao, Y. Han, X. Gao, L. Ma, S. Yuan, X. Ma, J. Zhou, X. Feng and B. Wang, *J. Am. Chem. Soc.* 2017, **139**, 4258-4261.
145. F. Haase, E. Troschke, G. Savasci, T. Banerjee, V. Duppel, S. Dörfler, M. M. J. Grundei, A. M. Burow, C. Ochsenfeld, S. Kaskel and B. V. Lotsch, *Nat. Commun.* 2018, **9**, 2600.
146. X. Li, C. Zhang, S. Cai, X. Lei, V. Altoe, F. Hong, J. J. Urban, J. Ciston, E. M. Chan and Y. Liu, *Nat. Commun.* 2018, **9**, 2998.
147. Q. Jiang, Y. Li, X. Zhao, P. Xiong, X. Yu, Y. Xu and L. Chen, *J. Mater. Chem. A* 2018, **6**, 17977-17981.
148. Y. Wu, Z. Zhang, S. Bandow and K. Awaga, *Bull. Chem. Soc. Jpn*, 2017, **90**, 1382-1387.
149. D.-G. Wang, N. Li, Y. Hu, S. Wan, M. Song, G. Yu, Y. Jin, W. Wei, K. Han, G.-C. Kuang and W. Zhang, *ACS Appl. Mater. Interfaces* 2018, **10**, 42233-42240.
150. C. Qian, Q.-Y. Qi, G.-F. Jiang, F.-Z Cui, Y. Tian and X. Zhao, *J. Am. Chem. Soc.* 2017, **139**, 6736-6743.
151. G. Zhang, M. Tsujimoto, D. Packwood, N. T. Duong, Y. Nishiyama, K. Kadota, S. Kitagawa and S. Horike, *J. Am. Chem. Soc.* 2018, **140**, 2602-2609.
152. H.-L. Qian, Y. Li and X.-P Yan, *J. Mater. Chem. A* 2018, **6**, 17307-17311.
153. P. J. Waller, Y. S. AlFaraj, C. S. Diercks, N. N. Jarenwattananon and O. M. Yaghi, *J. Am. Chem. Soc.* 2018, **140**, 9099-9103.

154. M. C. Daugherty, E. Vitaku, R. L. Li, A. M. Evans, A. D. Chavez and W. R. Dichtel, *Chem. Commun.* 2019, **55**, 2680-2683.
155. M. R. Rao, Y. Fang, S. De Feyter and D. F. Perpichka, *J. Am. Chem. Soc.* 2017, **139**, 2421-2427.
156. Q. Fang, J. Wang, S. Gu, R. B. Kaspar, Z. Zhuang, J. Zheng, H. Guo, S. Qiu and Y. Yan, *J. Am. Chem. Soc.* 2015, **137**, 8352-8355.
157. L. Bai, S. Z. Phua, W. Q. Lim, A. Jana, Z. Luo, H. P. Tham, L. Zhao, Q. Gao and Y. Zhao, *Chem. Commun.* 2016, **52**, 4128-4131.
158. S. Mitra, H. S. Sasmal, T. Kundu, S. Kandambeth, K. Illath, D. D. Díaz and R. Banerjee, *J. Am. Chem. Soc.* 2017, **139**, 4513-4520.
159. V. S. Vyas, M. Vishwakarma, I. Moudrakovski, F. Haase, G. Savasci, C. Ochsenfeld, J. P. Spatz and B. V. Lotsch, *Adv. Mater.* 2016, **28**, 8749-8754.
160. P. Bhanja, S. Mishra, K. Manna, A. Mallick, K. Das Saha and A. Bhaumik, *ACS Appl. Mater. Interfaces* 2017, **9**, 31411-31423.
161. S. Kandambeth, V. Venkatesh, D. B. Shinde, S. Kumari, A. Halder, S. Verma and R. Banerjee, *Nat. Commun.* 2015, **6**, 6786.
162. S. Zhang, Y. Zheng, H. An, B. Aguila, C.-X. Yang, Y. Dong, W. Xie, P. Cheng, Z. Zhang, Y. Chen and S. Ma, *Angew. Chem. Int. Ed.* 2018, **57**, 16754-16759.
163. Q. Sun, C.-W. Fu, B. Aguila, J. Perman, S. Wang, H.-Y. Huang, F.-S. Xiao and S. Ma, *J. Am. Chem. Soc.* 2018, **140**, 984-992.
164. J. Tan, S. Namuangruk, W. Kong, N. Kungwan, J. Guo and C. Wang, *Angew. Chem. Int. Ed.* 2016, **55**, 13979-13984.

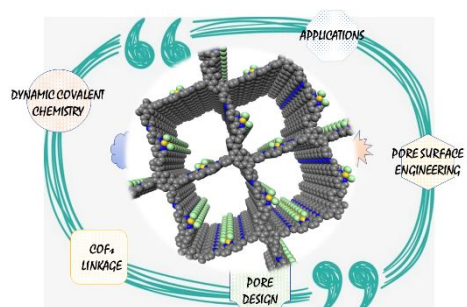
165. X. Zheng, L. Wang, Q. Pei, S. He, S. Liu and Z. Xie, *Chem. Mater.* 2017, **29**, 2374-2381.
166. S. Mitra, S. Kandambeth, B. P. Biswal, M. A. Khayum, C. K. Choudhury, M. Mehta, G. Kaur, S. Banerjee, A. Prabhune, S. Verma, S. Roy, U. K. Kharul and R. Banerjee, *J. Am. Chem. Soc.* 2016, **138**, 2823-2828.
167. Q. Fang, S. Gu, J. Zheng, Z. Zhuang, S. Qiu and Y. Yan, *Angew. Chem. Int. Ed.* 2014, **53**, 2878-2882.
168. Y. Peng, Z. Hu, Y. Gao, D. Yuan, Z. Kang, Y. Qian, N. Yan and D. Zhao, *ChemSusChem* 2015, **8**, 3208-3212.
169. S. Lin, C. S. Diercks, Y.-B. Zhang, N. Kornienko, E. M. Nichols, Y. Zhao, A. R. Paris, D. Kim, P. Yang, O. M. Yaghi and C. J. Chang, *Science* 2015, **349**, 1208-1213.
170. V. Saptal, D. B. Shinde, R. Banerjee and B. M. Bhanage, *Catal. Sci. Technol.* 2016, **6**, 6152-6158.
171. X. Wang, X. Han, J. Zheng, X. Wu, Y. Liu and Y. Cui, *J. Am. Chem. Soc.* 2016, **138**, 12332-12335.
172. D. B. Shinde, S. Kandambeth, P. Pachfule, R. R. Kumar and R. Banerjee, *Chem. Commun.* 2015, **51**, 310-313.
173. X. Li, Z. Wang, J. Sun, J. Gao, Y. Zhao, P. Cheng, B. Aguila, S. Ma, Y. Chen, Z. Zhang, *Chem. Commun.* 2019, **55**, 5423-5426.
174. V. S. Vyas, F. Haase, L. Stegbauer, G. Savasci, F. Podjaski, C. Ochsenfeld and B. V. Lotsch, *Nat. Commun.* 2015, **6**, 8505.

175. T. Sick, A. G. Hufnagel, J. Kampmann, I. Kondofersky, M. Calik, J. M. Rotter, A. Evans, M. Döblinger, S. Herbert, K. Peters, D. Böhm, P. Knochel, D. D. Medina, D. Fattakhova-Rohlfing and T. Bein, *J. Am. Chem. Soc.* 2018, **140**, 2085-2092.
176. J. Thote, H. B. Aiyappa, A. Deshpande, D. D. Díaz, S. Kurungot and R. Banerjee, *Chem.-Eur. J.* 2014, **20**, 15961-15965.
177. S.-Y. Ding, M. Dong, Y.-W. Wang, Y.-T. Chen, H.-Z. Wang, C.-Y Su and W. Wang, *J. Am. Chem. Soc.* 2016, **138**, 3031-3037.
178. N. Huang, L. Zhai, H. Xu and D. Jiang, *J. Am. Chem. Soc.* 2017, **139**, 2428-2434.
179. Z. Li, H. Li, X. Guan, J. Tang, Y. Yusran, Z. Li, M. Xue, Q. Fang, Y. Yan, V. Valtchev and S. Qiu, *J. Am. Chem. Soc.* 2017, **139**, 17771-17774.
180. G. Das, T. Skorjanc, S. K. Sharma, F. Gándara, M. Lusi, D. S. S. Rao, S. Vimala, S. K. Prasad, J. Raya, M. Lusi, D. S. Han, R. Jagannathan, J.-C. Oslen and A. Trabolsi, *J. Am. Chem. Soc.* 2017, **139**, 9558-9565.
181. N. Huang, P. Wang, M. A. Addicoat, T. Heine and D. Jiang, *Angew. Chem. Int. Ed.* 2017, **56**, 4982-4986.
182. G.-H Ning, Z. Chen, Q. Gao, W. Tang, Z. Chen, C. Liu, B. Tian, X. Li, K. P. Loh, *J. Am. Chem. Soc.* 2017, **139**, 8897-8904.
183. H. Furukawa and O. M. Yaghi, *J. Am. Chem. Soc.* 2009, **131**, 8875-8883.
184. H. Li, Q. Pan, Y. Ma, X. Guan, M. Xue, Q. Fang, Y. Yan, V. Valtchev and S. Qiu, *J. Am. Chem. Soc.* 2016, **138**, 14783-14788.
185. S. B. Kalidindi and R. A. Fischer, *Phys. Status Solidi B* 2013, **250**, 1119-1127.
186. Y. Zeng, R. Zou and Y. Zhao, *Adv. Mater.* 2016, **28**, 2855-2873.

187. C. J. Doonan, D. J. Tranchemontagne, T. G. Glover, J. R. Hunt and O. M. Yaghi, *Nat. Chem.* 2010, **2**, 235-238.
188. H. Ma, H. Ren, S. Meng, Z. Yan, H. Zhao, F. Sun and G. Zhu, *Chem. Commun.* 2013, **49**, 9773-9775.
189. S.-L Cai, K. Zhang, J.-B. Tan, S. Wang, S.-R Zheng, J. Fan, Y. Yu, W.-G. Zhang and Y. Liu, *ACS Macro Lett.* 2016, **5**, 1348-1352.
190. Z. Li, X. Feng, Y. Zou, Y. Zhang, H. Xia, X. Liu and Y. Mu, *Chem. Commun.* 2014, **50**, 13825-13828.
191. G. Lin, H. Ding, D. Yuan, B. Wang and C. Wang, *J. Am. Chem. Soc.* 2016, **138**, 3302-3305.
192. C. Zhang, S. Zhang, Y. Yan, F. Xia, A. Huang and Y. Xian, *ACS Appl. Mater. Interfaces* 2017, **9**, 13415-13421.
193. Y.-F. Xie, S.-Y. Ding, J.-M. Liu, W. Wang and Q.-Y. Zheng, *J. Mater. Chem. C* 2015, **3**, 10066-10069.
194. G. Das, B. P. Biswal, S. Kandambeth, V. Venkatesh, G. Kaur, M. Addicoat, T. Heine, S. Verma and R. Banerjee, *Chem. Sci.* 2015, **6**, 3931-3939.
195. Z. Li, Y. Zhang, H. Xia, Y. Mu and X. Liu, *Chem. Commun.* 2016, **52**, 6613-
196. Y. Peng, Y. Huang, Y. Zhu, B. Chen, L. Wang, Z. Lai, Z. Zhang, M. Zhao, C. Tan, N. Yang, F. Shao, Y. Han and H. Zhang, *J. Am. Chem. Soc.* 2017, **139**, 8698-8704.
197. A. Mal, R. K. Mishra, V. K. Praveen, M. A. Khayum, R. Banerjee and A. Ajayaghosh, *Angew. Chem. Int. Ed.* 2018, **57**, 8443-8447.
198. S. Wan, J. Guo, J. Kim, H. Ihee and D. Jiang, *Angew. Chem. Int. Ed.* 2009, **48**, 5439-5442.

199. X. Feng, L. Chen, Y. Honsho, O. Saengsawang, L. Liu, L. Wang, A. Saeki, S. Irle, S. Seki, Y. Dong and D. Jiang, *Adv. Mater.* 2012, **24**, 3026-3031.
200. M. Dogru, M. Handloser, F. Auras, T. Kunz, D. Medina, A. Hartschuh, P. Knochel and T. Bein, *Angew. Chem. Int. Ed.* 2013, **52**, 2920-2924.
201. Y. Zhang, J. Duan, D. Ma, P. Li, S. Li, H. Li, J. Zhou, X. Ma, X. Feng and B. Wang, *Angew. Chem. Int. Ed.* 2017, **56**, 16313-16317.
202. Q. Xu, S. Tao, Q. Jiang and D. Jiang, *J. Am. Chem. Soc.* 2018, **140**, 7429-7432.
203. S. Chandra, T. Kundu, S. Kandambeth, R. BabaRao, Y. Marathe, S. M. Kunjir and R. Banerjee, *J. Am. Chem. Soc.* 2014, **136**, 6570-6573.
204. H. Ma, B. Liu, B. Lin, L. Zhang, Y.-G. Li, H.-Q. Tan, H.-Y. Zang and G. Zhu, *J. Am. Chem. Soc.* 2016, **138**, 5897-5903.
205. C. R. DeBlase, K. E. Silberstein, T.-T. Truong, H. D. Abruna and W. R. Dichtel, *J. Am. Chem. Soc.* 2013, **135**, 16821-16824.
206. C. R. Mulzer, L. Shen, R. P. Bisbey, J. R. McKone, N. Zhang, H. D. Abruna and W. R. Dichtel, *ACS Cent. Sci.* 2016, **2**, 667-673.
207. J. W. Colson, A. R. Woll, A. Mukherjee, M. P. Levendorf, E. L. Spitler, V. B. Shields, M. G. Spencer, J. Park and W. R. Dichtel, *Science* 2011, **332**, 228-231.
208. E. L. Spitler, J. W. Colson, F. J. Uribe-Romo, A. R. Woll, M. R. Giovino, A. Saldivar, W. R. Dichtel, *Angew. Chem. Int. Ed.* 2012, **51**, 2623-2627.
209. D. D. Medina, M. L. Petrus, A. N. Jumabekov, J. T. Margraf, S. Weinberger, J. M. Rotter, T. Clark and T. Bein, *ACS Nano* 2017, **11**, 2706-2713.
210. Q. Hao, C. Zhao, B. Sun, C. Lu, J. Liu, M. Liu, L.-J. Wan and D. Wang, *J. Am. Chem. Soc.* 2018, **140**, 12152-12158.

211. J. Lv, Y.-X. Tan, J. Xie, R. Yang, M. Yu, S. Sun, M.-D. Li, D. Yuan and Y. Wang, *Angew. Chem. Int. Ed.* 2018, **57**, 12716-12720.
212. R. Chen, J.-L. Shi, Y. Ma, G. Lin, X. Lang and C. Wang, *Angew. Chem. Int. Ed.* 2019, **58**, 6430-6434.
213. C. Wu, Y. Liu, H. Liu, C. Duan, Q. Pan, J. Zhu, F. Hu, X. Ma, T. Jiu, Z. Li and Y. Zhao, *J. Am. Chem. Soc.* 2018, **140**, 10016-10024.



The review article summarizes recent progress in the pore surface engineering of covalent organic frameworks (COFs) for various applications.